

Philips Technical Review

DEALING WITH TECHNICAL PROBLEMS

RELATING TO THE PRODUCTS, PROCESSES AND INVESTIGATIONS OF

N.V. PHILIPS' GLOEILAMPENFABRIEKEN

EDITED BY THE RESEARCH LABORATORY OF N.V. PHILIPS' GLOEILAMPENFABRIEKEN, EINDHOVEN, HOLLAND

ELECTRON-OPTICAL OBSERVATIONS ON THE TRANSITION OF ALPHA TO GAMMA IRON

By W. G. BURGERS and J. J. A. PLOOS VAN AMSTEL

Summary. To investigate the process of transformation or recrystallisation in a metal by the standard etching method used in metallography, etching must in general be performed during the transformation itself. In most instances this introduces considerable difficulty, particularly at high transformation temperatures. In such cases the electron-optical method of exhibiting the crystal structure of a metal at a high temperature can prove of great service. The present article describes how this procedure may be applied to the investigation of the transformation of iron from the γ to the α phase which occurs at about 900°C .

In the previous issue¹⁾ of this Review it was shown how the crystalline structure of a heated metal surface could be rendered visible by electron-optical means in the cathode ray tube. This method consists in focusing the electrons emitted from the metal acting as a cathode, on to a fluorescent screen in the tube by applying suitable electrical and magnetic fields to the electron beam. A fluorescent image is produced on the screen whose brightness corresponds point for point to the emitting cathode surface and which can moreover be enlarged to give a much magnified image of this surface. Since the individual crystals of which the cathode is composed in general emit electrons to a varying degree owing to differences in composition and axial orientation, fluorescent areas of varying intensity are produced on the screen. The screen thus reveals a pattern very similar to an etched figure, a feature very aptly shown in fig. 6 of the previous paper.

This method of rendering visible the crystalline structure of a metal specimen at a high temperature can prove particularly instructive where the metal undergoes a transformation on heating and it is

desirable to investigate the stable phase above the transition point. By the etching process commonly used in metallography and briefly outlined in the previous article, this can only be done by etching at room temperature when the phase in question can be supercooled by reducing the temperature of the heated testpiece at a sufficient velocity ("quenching"). But frequently retention of this phase is impossible even on the most rapid cooling. In order to investigate in such case the phase existing at a high temperature the testpiece must be etched at this temperature.

That the etched figure then obtained remains stable in spite of the transformation occurring during cooling is demonstrated by the following. As already explained in the previous article the surface of the crystallites becomes "stepped" as a result of etching. These steps are of "microscopic size", i.e. they are composed of a large number of atoms, and their direction conforms with specific surfaces of the crystal lattice. An etched surface of this type is again reproduced in fig. 1 with the crystals shown by continuous lines. Assume that the crystals owing to a transformation during cooling have been altered to the state as shown by the broken lines. In general these changes are not directly observable, for as the alterations in structure in many cases take place atom for atom, the new crystals completely occupy the same space as previously taken up by the original crystals, except for deviations of atomic dimensions (approx. 10^{-8} cm) at the surface. These

¹⁾ Philips techn. Rev., 1, 312, 1936.

changes are however much too small to alter the visible shape of the steps, so that no difference is detected in the etched figure²⁾. Only on further etching does the old surface disappear and in place of it there appears a surface formed by the newly-constituted crystals.

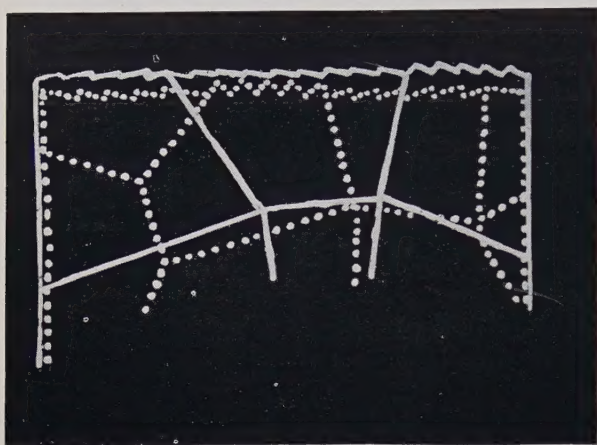


Fig. 1. Structural changes in a metal during recrystallisation (diagrammatic representation after van Arkel and Koets). The figure shows a section drawn perpendicular to the surface of the test specimen. The continuous lines indicate the boundaries of the crystals originally present, at which a step-shaped surface is exposed by etching. The crystals produced by transformation and indicated by broken lines completely fill the space occupied by the previous phase, except for differences of atomic dimensions (of a magnitude of 10^{-8} cm). Only after renewed etching is the old step-shaped surface displaced by one corresponding to the new crystals formed, so that the latter becomes apparent.

In many cases the etching of surfaces at a high temperature is a difficult matter, particularly where not only the phase formed by a specific transformation, but also the development of such transformation itself is to be studied.

The intrinsic suitability of the electron-optical method for investigating a transformation taking place at a high temperature is shown by the study described below of the transformation of the alpha modification of iron stable at temperatures below about 900°C into the gamma modification³⁾ stable above this temperature.

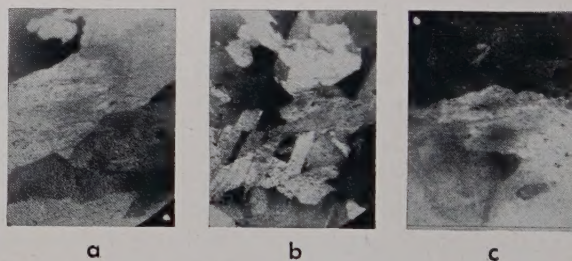


Fig. 2. Electron-optical images of crystal structure (magnification approx. 15) of a heated iron strip whose temperature is a) a little above, b) a little below, and c) again above the transformation temperature of the two modifications. The figures thus show: a) γ crystals, b) α crystals, and c) again γ crystals. Figures a and c are seen to be quite different.

during a period of 10 minutes and could be successfully photographed with a standard film camera (through the glass plate *b* in fig. 3, loc. cit.) employing an exposure time of about 2 secs.

The mechanism of activation on these lines has

⁴⁾ E. Brüche and W. Knecht, Z. techn. Phys., 15, 461, 1934; 16, 95, 1935.

⁵⁾ These investigations could however quite definitely conclude from the alteration in the crystal pattern, if any, whether the transformation point was passed or not on reducing the temperature, by making all observations at 1000°C . and reducing the cathode temperature for a short time between successive observations to a temperature in the neighbourhood of the transformation point.

²⁾ There are however exceptions. So the growth of martensite needles can immediately be observed without etching. This transformation was cinematographically recorded by H. J. Wiester, Z. Metallk., 24, 276, 1932.

³⁾ As is well known the iron atoms in both modifications form a cubic lattice, with the sole difference that in the case of α iron the centres of the cubic cells are occupied in addition to the corners (space-centred structure), while in γ iron the cubic surfaces are occupied in addition to the corners (face-centred structure). That the modification stable above 900°C is denoted by γ and not by β is associated with the fact that magnetic α iron stable at room temperature becomes non-magnetic at about 760°C (Curie point) and this non-magnetic phase, which has the same crystal structure as the magnetic phase, is already designated as β iron. It would in fact be more logical to term the transformation at 900°C the β -transformation.

already been described in detail in the previous article on the basis of a series of photographic records. The photographs reproduced in fig. 5 of that article relate to iron. In fig. 2 of the present article three crystal-structure patterns obtained by the same method are reproduced. These were obtained with the same strip and at temperatures just above, just below and also directly at the transformation point. The patterns thus show in 15-fold magnification: a) γ crystals, b) α crystals, and c) again γ crystals. From a metallographic standpoint the fact is interesting that the two γ structures are different: The first transformation from the γ into the α phase was probably very complete and left no γ nuclei, which on subsequent transformation could have caused the re-generation of the original crystals.

The progress of transformation itself can also be very well followed by varying the electric current passing through the iron when the latter is heated in the neighbourhood of the transformation point. The occurrence of a temperature gradient in the strip (as a result of the marked cooling at the clamped ends) causes a displacement along the surface of the strip of the line of separation between the crystalline states above and below the transformation temperature. In consequence transformation is seen to proceed from one side of the fluorescent screen to the other. By very slowly altering the current the duration of transformation could be extended to a period of 5 minutes, thus permitting the whole process to be filmed using an exposure time of 2 secs per picture as indicated above.

The observation of the transition of the γ phase stable above the transformation temperature into the α phase stable below this temperature was particularly successful. Since the ends of the strip are always at room temperature, α crystals are always present in the colder part of the strip; these serve as nuclei and ensure a uniform development of the transformation process. Conditions are however different on inverse transformation: At the beginning of the experiment γ crystals are then absent and it may occur that transformation is only initiated when some point or other is superheated to a few degrees. When this has once occurred the nuclei generated then frequently commence to grow suddenly and very rapidly (owing to the high temperature) and it is no longer possible to register the development of growth photographically using the comparatively long exposure time of 2 secs per picture.

In figs. 3 and 4 two series of photographs taken from a film are reproduced which bring out well the transition of γ crystals into α crystals. A point to be noted is how the nuclei of the α phase formed on the left develop into more or less elongated

crystals filling the whole strip. The rate of growth of these crystals has thus kept pace with the velocity of transformation, so that practically no other nuclei are formed. The photographs, which are in fact enlargements of standard film pictures, show the crystal structure with a magnification of approx. 20 (fig. 3) and approx. 35 (fig. 4). The photographs in fig. 3 were made at the beginning of the investigation, i.e. before sufficient attention has been given to setting up the cathode ray tube on a vibrationless base, which thus accounts for their somewhat blurred appearance. This defect has in the meantime been eliminated. Fig. 4 with a still higher magnification demonstrates extremely well the suitability of the electron-optical method for investigating the transformation processes. Further investigation of this method of analysis will show how far the procedure can prove of general application.

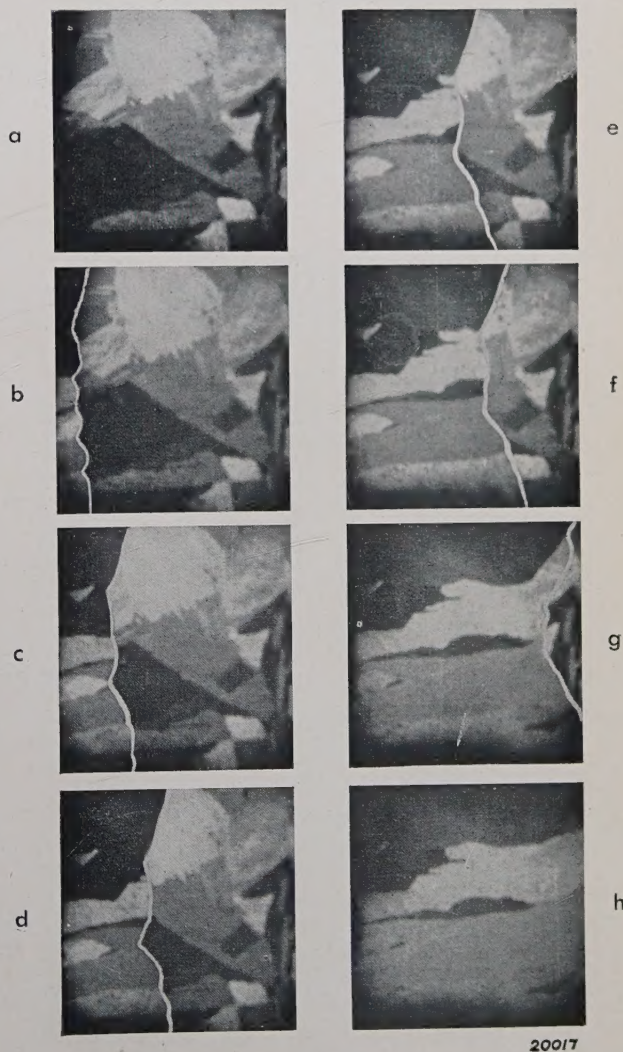


Fig. 3. Electron-optical representation of the transformation of γ crystals a) stable above 900°C into α crystals b) stable below 900°C on slowly lowering the temperature of the strip. The new crystals grow from left to right, as indicated by the white line of separation.

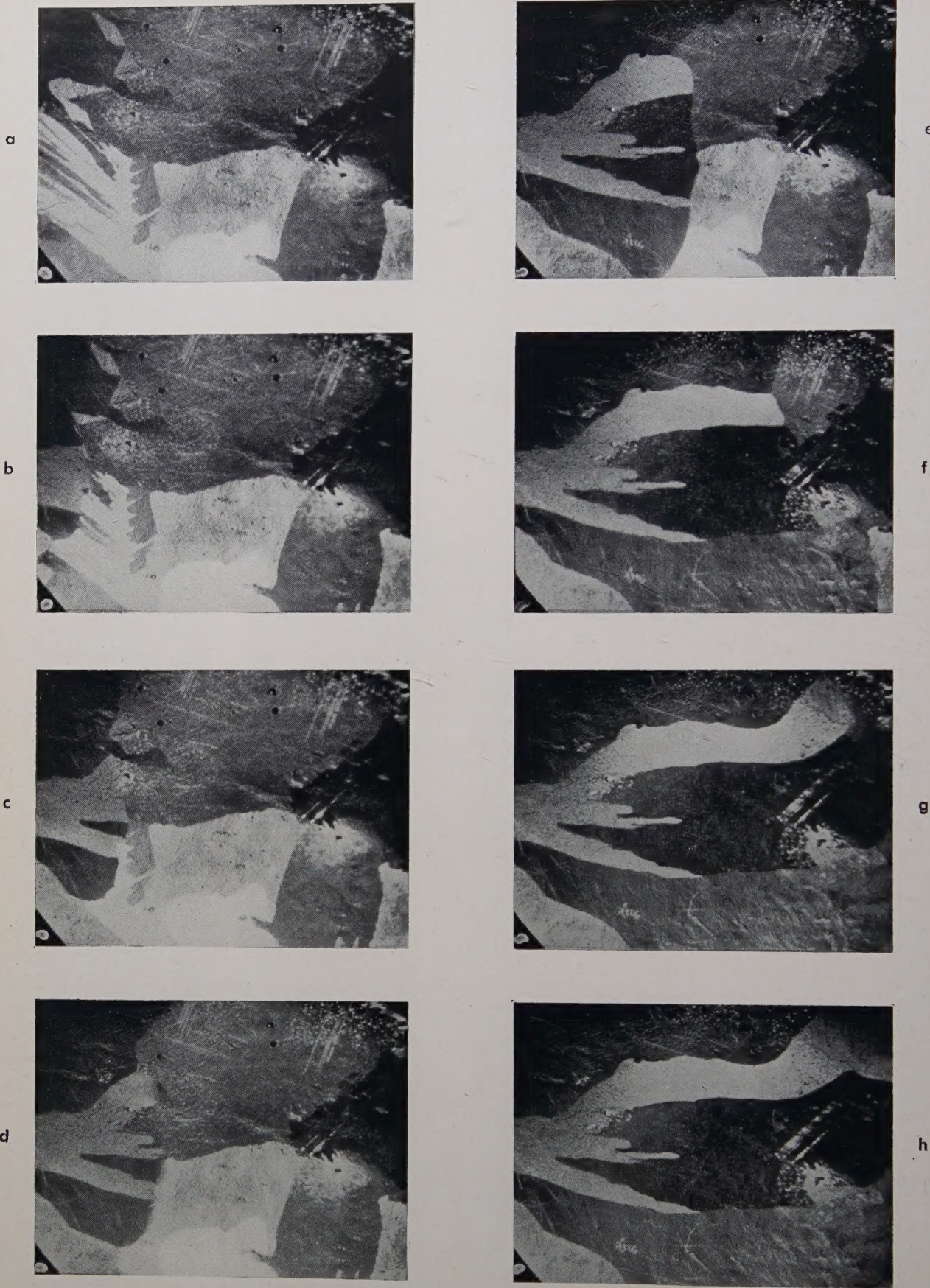


Fig. 4. As fig. 3. The line of separation between the growing α and the disappearing γ crystals is not shown here, since it can be quite clearly picked out.

20018

TELEVISION

by J. VAN DER MARK.

Summary. The television transmitter in the Philips Laboratory which has already been described in the first number of this review ¹⁾ has now been adapted for transmitting with a wide variety of line frequencies using sequential and interlaced scanning systems. These extensions are discussed, as well as a number of circuit details which were not referred to in the first article.

In a previous article ¹⁾ in this Review the television transmitter in this Laboratory has already been described in broad outline. In the present article details are given of a number of points on which further information has been gathered during experience with the experimental transmitter.

It should be pointed out at the outset that the transmitter in its present form, as indeed already indicated in the previous article, is suitable for transmitting purposes employing a wide choice of scanning lines per picture. Before passing to a closer consideration of this point we shall again briefly describe the scanning process employed.

The earlier description related to a unit for transmitting 25 pictures per second and 180 lines per picture. These pictures were on the whole quite satisfactory, but suffered from a very undesirable defect, viz., the bright parts in the field of vision were subject to flicker. This flickering produced an unsteady visual impression which made it very fatiguing to view the pictures for any length of time. The reason for this was that when an adequate brightness of the field of view was obtained the picture frequency of 25 per second was insufficient to produce a perfectly steady impression. This flickering could be avoided by transmitting at a higher picture frequency, e.g. 50 pictures per second, at which no fluctuations in the brightness impression occur ²⁾, but this would mean doubling the maximum modulation frequency to retain the same picture definition: a very undesirable alteration.

Flickering can, however, be suppressed without altering the maximum modulation frequency, viz., by adopting a suitable artifice. For if with an odd number of scanning lines per picture, e.g. 405, at a picture frequency of 25 per second, the picture frequency is doubled, i.e. to 50, then

202.5 scanning lines per picture will be obtained, i.e. not an integral number of lines. The scanning of the picture then commences alternately in the left-hand top corner and in the middle of the top edge of the picture. *Fig. 1* shows that this results in bringing the lines of the "even" pictures exactly

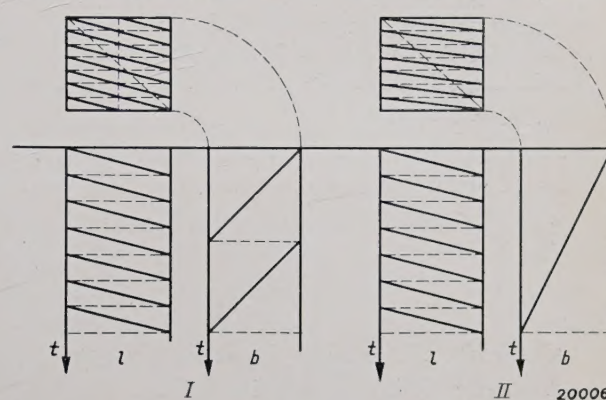


Fig. 1. Interlaced and sequential scanning of a picture of 7 lines. Both systems employ the same saw-tooth movement in scanning the lines (*I l* and *II l*); in interlaced scanning the saw-tooth movement of the lines across the frame has double the frequency as in sequential scanning (*I b* and *II b*). The net result is that by both systems the whole surface of the frame is scanned in the same time; with sequential scanning (right) the lines are scanned in direct succession, while in interlaced scanning (left) first all odd lines and then all even lines are scanned.

midway between the lines of the "odd" pictures. Although the whole picture surface is written in $1/25$ of a second, i.e. in the same time as formerly, directly contiguous lines in the picture are now reproduced alternately at intervals of $1/50$ of a second. Since a televised picture must be viewed from such a distance that the individual lines cannot be seen separately (in the same way as the impression of a screen block must be viewed from such a distance that the screen dots are not seen individually), no flickering will be observable. This effect is shown in *fig. 1* for a picture with only 7 lines.

The maximum modulation frequency in this system of scanning, called interleaved scanning, interlacing or line jump scanning, remains unchanged, for the number of

¹⁾ Philips techn. Rev., 1, 16, 1936.

²⁾ For reasons given later on in this article, there is in practice only a choice between 25 and 50 pictures per second when using a mains frequency of 50 cycles.

picture elements transmitted per second is not increased.

The transmitting equipment at the present moment is suitable for the use of the following scanning systems:

	Picture frequency per second	Scanning lines per picture	Scanning system	Picture
1)	50	90	Sequential	Non-flicker
2)	50	120	"	"
3)	50	180	"	"
4)	25	180	"	Flickering
5)	25	240	"	"
6)	25	360	"	"
7)	25	375	"	"
8)	25	405	"	"
9)	2×25	$187\frac{1}{2}$	Interlaced	Non-flicker
10)	2×25	$202\frac{1}{2}$	"	"

A number of examples is reproduced in *fig. 2*.

The oscillator, the frequency demultiplier and the various saw-tooth generators are adjusted by switches to the various requisite frequencies, so that by switching over a number of knobs a change can be made instantaneously from one system of scanning to the other.

In the diagrammatic sketch in *fig. 3*, a number of additional components not included in the previous layout (page 19 of this Review) are shown on the left next to the oscillator and the frequency demultiplication stages. The need for these auxiliaries is shown by the following considerations. The television receiver, and in fact also the transmitter, must be fed from the mains. The direct voltages employed, which are generated by rectification, will always indicate their origin by the presence of ripples, if no costly additional apparatus is included to avoid this effect, these ripples are apparent in the images by one or more slightly dark bands and a slight displacement of the lines. As long as the bands are stationary with respect to the frame, this effect can be tolerated, but the bands constitute a serious disturbance as soon as they commence to wander across the picture. Stationary bands are only obtained by synchronising the picture frequency with the A.C. mains supply. If interlaced scanning is used for transmission, synchronising becomes still more imperative, since adjoining lines are not scanned in direct succession, so that without synchronising the lines of the odd and the even pictures will move with respect to each other, the definition of the picture naturally suffering in consequence. If scanning is synchronised with the A.C., the two frames used with interlaced scanning follow each other at intervals of $1/50$ of a sec., as indicated in the table, i.e. with the same periodicity as the mains supply, with the

result that the adjoining lines are distorted to the same extent by the voltage ripple. It is also essential to synchronise the picture frequency with the mains also when transmitting films in which the projector is driven by a synchronous motor.



a)

20013



b)

20019



c)

20014

Fig. 2 Pictures obtained with: a) 90 lines, b) 180 lines, c) 405 lines

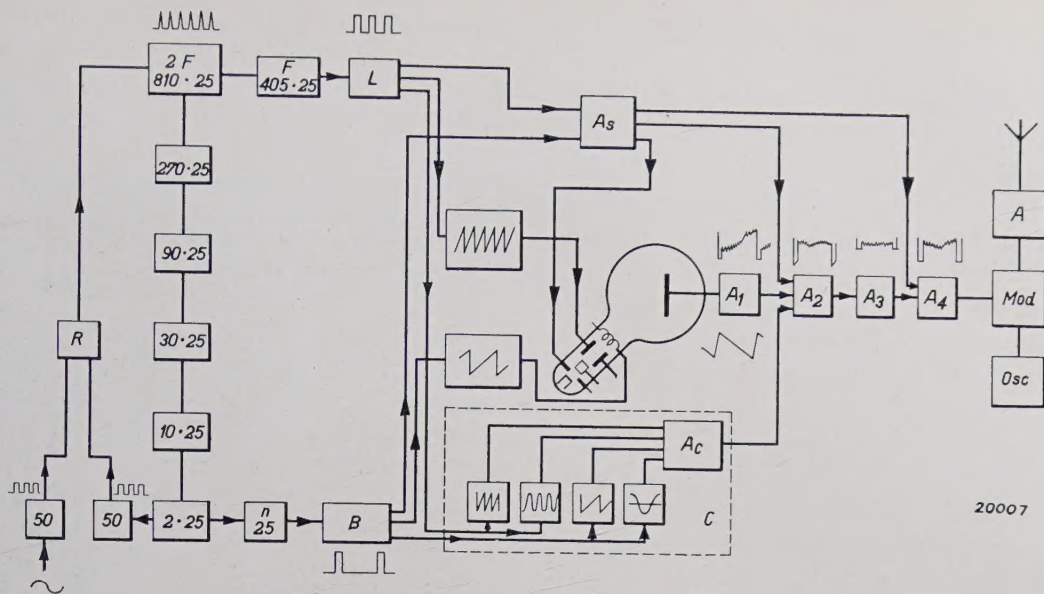


Fig. 3. Diagrammatic layout of the transmitter. In the oscillator $2F$ in the top left, impulses are generated with a frequency $2f$ (f is the line frequency, being equal to the product of the picture frequency n per second and the number of lines N per picture). In the stages depicted below this frequency is demultiplied until a 50-cycle frequency is obtained. In this way the picture frequency n (25 or 50 cycles) is arrived at on the one hand, and on the other hand (going to the left in the diagram) the oscillator, which furnishes a voltage with a rectangular time diagram, is controlled. This voltage, together with an equal mains-controlled voltage is passed to a component marked R ; the latter furnishes a direct voltage which is a measure of the phase difference between the two alternating voltages. This direct voltage serves as the control voltage for the oscillator $2F$ which in this way is stabilised as described in the text. The impulses furnished by F and n are converted in L and B to synchronising signals with rectangular voltage characteristics. These signals are mixed and amplified in the amplifier A_s ; they also serve for operating the two saw-tooth generators for controlling the electron beam in the iconoscope, and are finally passed to the complex C which furnishes the compensating signals. From the amplifier A_s the synchronising signals are *inter alia*, passed to the control electrode of the iconoscope in order to suppress the electron beam during each flyback. Four different compensating signals are given in the diagram (although actually more are used), viz., the saw-tooth voltages with line and picture frequencies, and sinusoidal voltages with the same frequencies. These voltages, each of which can be regulated, are mixed in the amplifier A_c . The picture signals of the iconoscope are first amplified in the amplifier A_1 . As shown diagrammatically these signals increase, for instance, from left to right, while they should have a horizontal mean value throughout. By mixing a suitable compensating signal from A_c in the amplifier A_2 , this horizontal level may be obtained. The end of the synchronising signal is however then distorted. To eliminate this distortion the distorted end is cut out in A_3 , by limiting the amplitude, whereupon a synchronising signal is added in A_4 in order to obtain the correct amplitude for the synchronising signal. The signal is then passed to the transmitter.

The frequency of the oscillator, which controls scanning, must therefore be of such a value that the picture frequency which is derived from it by a series of demultiplications is maintained in synchronism with the mains. This is done in the following way: The oscillator is designed on such lines that its frequency can be regulated within specific limits by altering a direct voltage. The latter is furnished by a circuit in which a 50-cycle alternating voltage derived from the mains is balanced against another 50-cycle alternating

voltage generated by frequency demultiplication. This circuit is so designed that the direct voltage obtained is a measure of the phase difference between these two voltages. As soon as the picture frequency deviates slightly from the mains frequency, this phase difference will be altered and hence also the direct voltage. This change in the direct voltage now reacts on the oscillator frequency in such a way that the initial change is compensated. In this way the line and picture impulses are maintained in a strict proportionality by demul-

tiplication in frequency and phase, and the latter are always synchronised with the mains supply and in a definite adjustable phase relationship with it.

The circuit diagram in fig. 3 also includes a number of other alterations whose purpose will also be described in some detail. It has already been indicated in the previous article that the iconoscope furnishes a voltage whose magnitude at every instant is a measure of the illumination incident on that part of the light-sensitive plate being scanned at that moment. In addition to this signal, the iconoscope can also generate a further, and undesirable, signal owing to a small part of the electrons emitted from the signal plate returning to it and impinging at points different from their initial points of emission. There thus results a charge transport from one part of the signal plate to other parts, such transport becoming apparent in the final picture as blurred bright and dark patches. The definition of the picture does not suffer in consequence, but the average brightness over certain areas deviates from the correct value. Since this phenomenon makes itself apparent as large blurred spots, it is possible to eliminate it by means of an auxiliary signal.

If, for instance, a picture is obtained at the receiver which is too bright on the left and too dark on the right, this condition can be improved by superposing in the transmitter a compensating signal in the form of a saw-tooth voltage with the line frequency on the voltage furnished by the iconoscope (the line frequency is entailed here since the lines are scanned from left to right). In this way the average brightness is reduced on the left and increased on the right, so that with a suitable choice of voltage the correct value is obtained over the whole frame. The result is checked with a monitor receiver.

To permit this method of compensation to be used in all cases, various compensating voltages are available, such as e.g. saw-tooth voltages of picture and line frequency and alternating voltages of various frequencies, which are derived from the synchronising impulses. As Fourier components the synchronising impulses contain a large number of harmonics of the picture and line frequencies. All these voltages can be continuously and controllably mixed or modulated with respect to each other, both in magnitude and direction, and impressed on the picture. Naturally the compensating signals must be subsequently regulated by hand, the result being checked on a monitor reproduction tube. It should also be noted that

by the addition of the compensating signals the synchronising signals become distorted, as shown in fig. 3 in the diagrams drawn above A_2 and A_4 . As this is not permissible if efficient

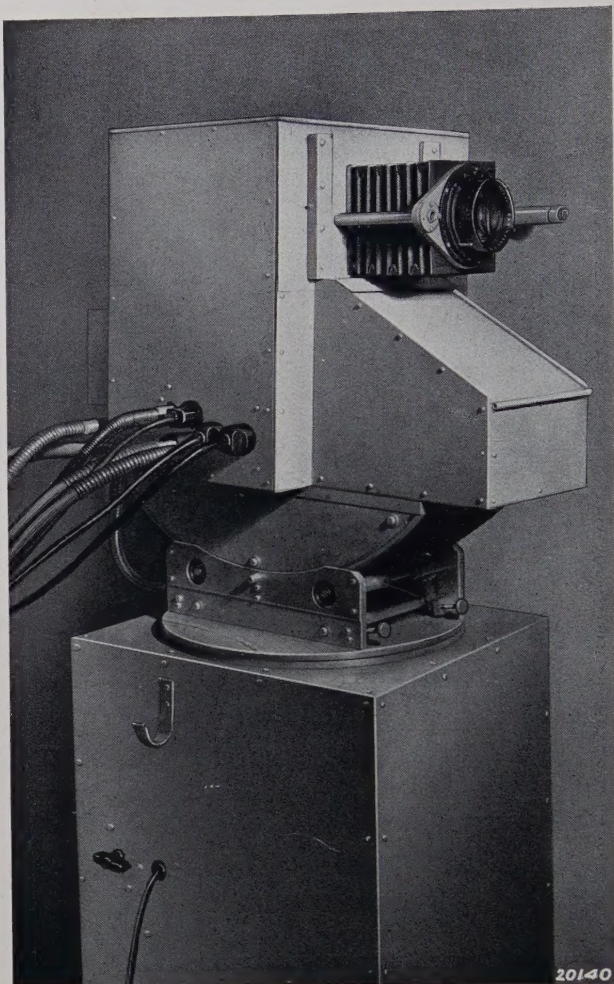


Fig. 4. Iconoscope camera.

operation of the receiver is to be ensured, the distorted part of the synchronising signals is eliminated in a special amplifier A_3 by limiting the amplitude, and after a new synchronising signal has been superposed in A_4 the total signal is then passed to the actual transmitter.

A small temporary transmitting room has been equipped in which the television camera was set up; the camera is as mobile as an ordinary film camera and is connected by cables with the feed-voltage supplies and the control board. The iconoscope was electrically controlled from this control board. By means of a mirror the cameraman is able to check directly the definition of the optical image on the iconoscope screen. Since the focal length of the lens is fairly large (21 cm) owing to the size of the iconoscope, the depth of contrast is very small with the diaphragm fully open ($f/2.9$),



Fig. 5. Filmprojector and iconoscope

so that focusing requires very great care. In this respect, the conditions are less satisfactory than when filming.

Regarding the sensitivity, it has been found that as a rule outdoor scenes which can be suitably filmed can also be satisfactory picked up with the iconoscope.

For direct-transmission from the transmitting room Philips water-cooled high-pressure mercury lamp was used as a light source. The general lighting was provided by a combination of three of these lamps, which owing to their compact dimensions could be placed close together; when fed from three-phase alternating-current mains this group gave a practically constant light output. (In television the light source must not be subject to fluctuation, as the various parts of the object

are reproduced in succession and light fluctuations are liable to appear as dark and bright strips.) The aggregate output of the group of three lamps referred to is 7.5 kilowatts.

Small mercury lamps were used as auxiliary lighting to illuminate areas in shadow.

This method of illumination represents an important advance, mainly because of the small amount of heat radiated. With incandescent lamps and arc lamps the radiation of heat is frequently intolerable to the speakers or artists being televised, while the mercury lamps radiate only very little heat. This is a very important point in television, since here the persons must usually face the camera for longer periods than when being filmed, where the individual scenes usually do not exceed more than a few minutes in duration.

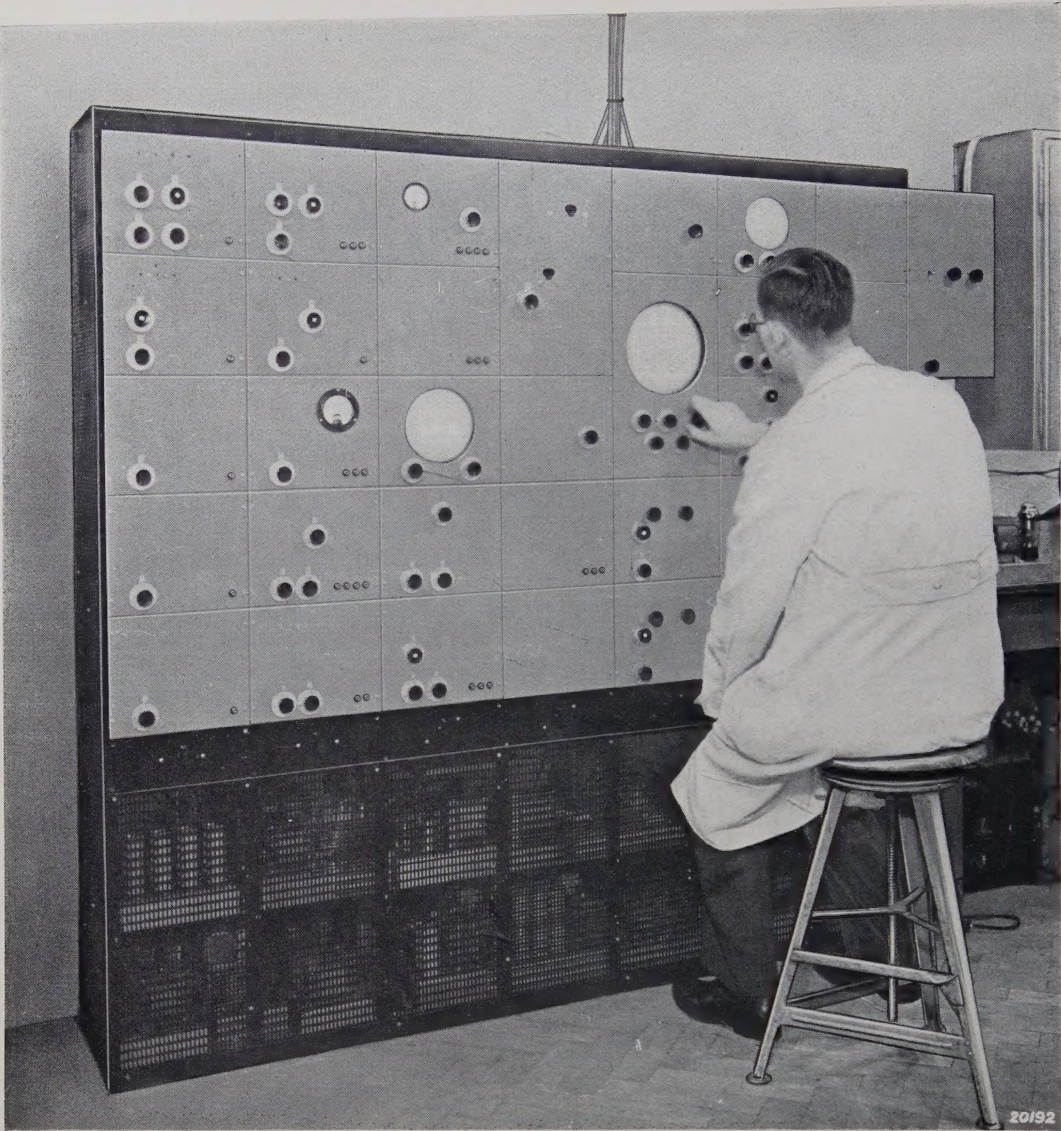


Fig. 6. Control board.

ELECTRICAL FILTERS IV

Vacation Course, held at Delft, April 1936

By BALTH. VAN DER POL and TH. J. WEIJERS.

HIGH-PASS AND BAND-PASS FILTER SECTIONS

Summary. The method described in the previous article for investigating low-pass filter sections (basic types and m -transformations) are applied in this article to high-pass and band-pass filters. Furthermore, in the section on "double m -transformation" an extension of the m -transformation is given, which can be applied to band-pass filters and, *inter alia*, can also give rise to sections of a particularly simple construction. All data obtained in this way for the design of low-pass, high-pass and band-pass filter sections are collated in Tables II and III. In conclusion, the design of a low-pass filter which has to meet specific requirements is discussed by way of example.

Basic Types and m -Transformations

In the previous articles it was shown how the image impedances, the propagation constant and the transmission and attenuation bands for T -sections, II -sections and half-sections could be represented as functions of the impedances Z_1 and Z_2 of the "complete branches".

Thus the transmission band is expressed by the condition that $Z_1/4Z_2$ must lie between -1 and 0 .

For the low-pass filter sections discussed in the previous article this condition was found to be satisfied for frequencies below a certain limiting frequency ν_1 . This condition may also be derived from the reactance diagrams of the fundamental types shown in *fig. 18*. The transmission band commences at the frequency 0 with $Z_1' = j0$ and $-4Z_2' = j\infty$. $Z_1' = j\omega L_1'$ increases with the frequency, $-4Z_2' = j4/\omega C_2'$ diminishes with increasing frequency; the point of intersection of the two curves determines the limiting frequency ν_1 .

These considerations also show the values which the impedances Z_1' and Z_2' must have in order to obtain a high-pass or a band-pass filter. For high-pass filter sections (*fig. 18b*) the transmission band reaches from the frequency ν_1 to ∞ , and for band-pass filter sections from ν_1 to ν_2 . In the case of all three basic types there is a frequency ν_0 for which $Z_1' = 0$ and $Z_2' = \infty$. For low-pass filter sections this frequency is 0 and for high-pass filter sections ∞ , while for the band-pass filter sections it is finite and lies between ν_1 and ν_2 .

The figure shows diagrammatically the variation of the reactances Z_1' and $-4Z_2'$, as a function of the frequency for the three basic types. The circuits of the complete branches giving these functions are shown at the side. In the case of the high-pass filter section Z_1' is a capacity C_1' , and Z_2' a self-inductance L_2' . With the band-pass filter section Z_1' is a self-inductance L_1' with a condenser C_1' in series, and Z_2' is a self-inductance L_2' with a

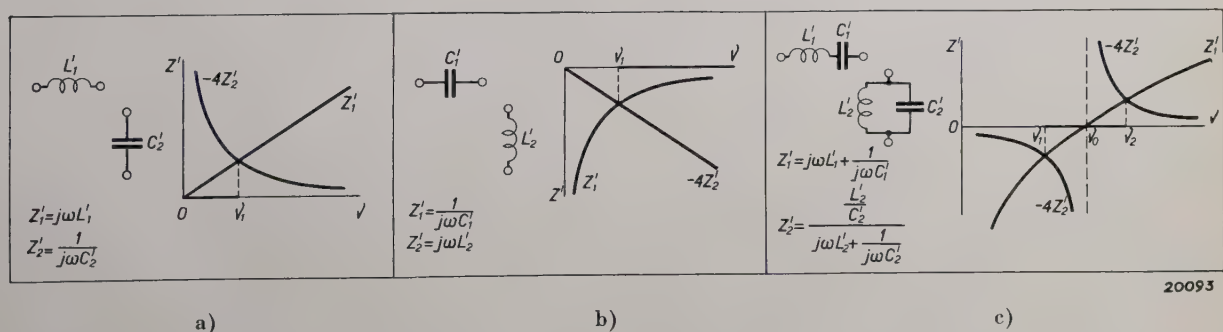


Fig. 18. Reactance diagrams. Reactances Z_1' and $-4Z_2'$ for filters of the basic type as a function of the frequency ν . a) Low-pass filter, b) High-pass filter, c) Band-pass filter. A filter has a passband when $-4Z_2'$ lies between Z_1' and the axis. The transmission bands are indicated on the axis by a thicker stroke. On the left of each diagram, it is indicated how the reactances can be made up from self-inductances and condensers and how they can be represented analytically as a function of the angular frequency.

condenser C_2' in parallel, where $L_1' C_1' = L_2' C_2'$ so that the impedance Z_2' becomes infinite at the same frequency ν_0 at which the impedance Z_1' disappears ¹⁾.

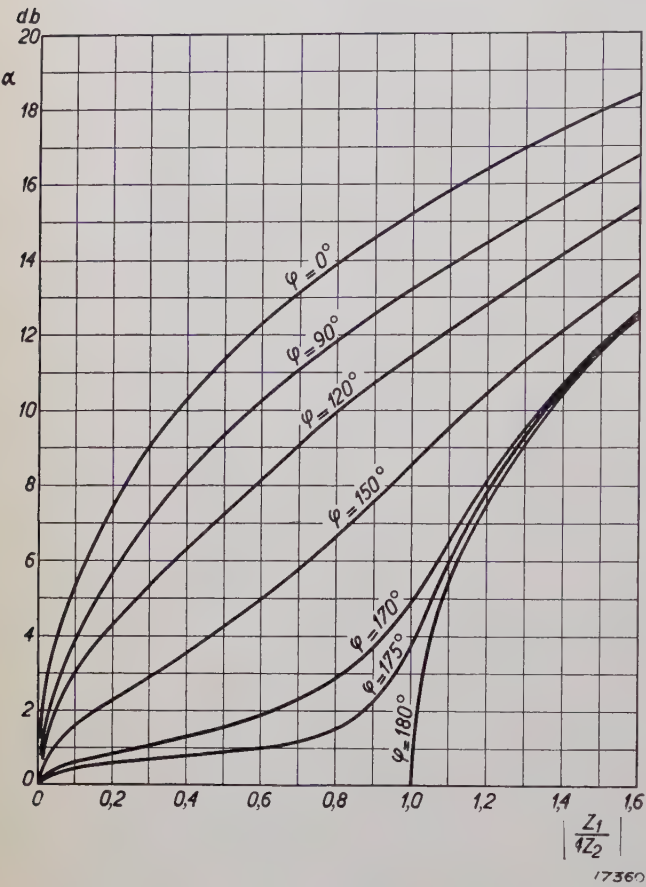


Fig. 19. Attenuation constant α (real component of the propagation constant T) in decibels expressed as a function of $|Z_1/4 Z_2|$ for T-sections and Π sections.

In the previous article (see e.g. p. 305, equation 9, 12, 15, 23, 24, 25, 29, 30 and 31) it was shown that the image impedances and the propagation constant could be expressed for all sections (basic types and m -transformations) in terms of $Z_1' Z_2'$ and $Z_1'/4 Z_2'$. Now for the low-pass, high-pass and band-pass filter sections of the basic type $Z_1' Z_2'$ has a real, positive value independent of the frequency, which in conformity with equation (36) in the previous article is denoted by R^2 . If now $Z_1'/4 Z_2'$ expressed as a function of the frequency is known for an arbitrary filter section of the basic type, then from the equations enumerated above the image impedances and the propagation constant can similarly be obtained as functions of

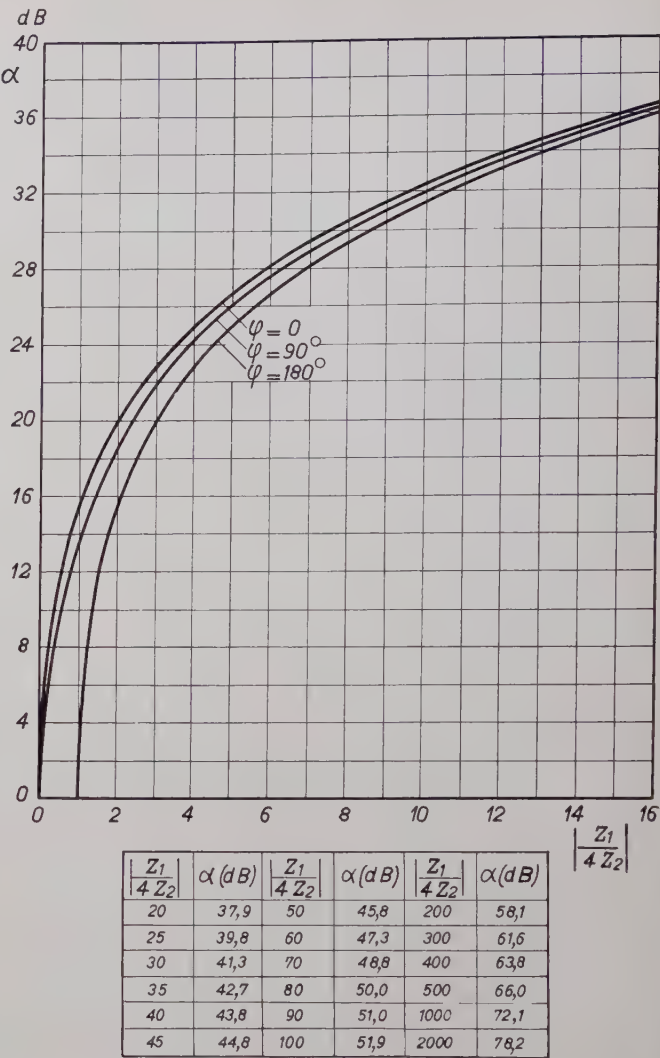


Fig. 20. Attenuation constant α in decibels for high values of $|Z_1/4 Z_2|$. For $|Z_1/4 Z_2| < 1.6$ fig. 19 is used. The table under the figure is a continuation of the graph for $|Z_1/4 Z_2| > 16$. In the latter case the effect of φ on α can be neglected in practice.

the frequency (hence also the transmission bands and the frequencies with infinite attenuation) for both the basic type and those types obtained after m -transformation.

The results obtained by this method have been collated in Table I. In addition the requisite data for laying out filters are also given in Tables II and III, on similar lines as already deduced for low-pass filter sections in the previous article (p. 304) ²⁾.

²⁾ These two tables are inserted in this issue of Philips techn. Rev. as separate sheets. The broken lines in the diagrams of the image impedances are intended to show that the image impedance is imaginary in the corresponding frequency band, being positive or negative according as the absolute value increases or decreases respectively with rising frequency.

¹⁾ If these frequencies are different, then $Z_1'/4 Z_2'$ will change its sign between ν_1 and ν_2 , and will therefore not lie wholly between 0 and -1 . Between the frequencies at which Z_1' and Z_2' become zero and infinity respectively, there is an attenuation band, which interrupts the transmission band.

All expressions in Table I, with the exception of the third line, apply for non-dissipative filter sections ($d = 0$). In the previous article (p. 302) a brief discussion was given on the effect of the losses in low-pass filter sections. The same remarks also apply to high-pass and band-pass filter sections.

The physical interpretation of the resistance $R = \sqrt{Z_1' Z_2'}$ was in the case of low-pass filter sections the image impedance (both Z_T and Z_π) at the frequency $\nu = 0$, and this was in fact true for both the basic type and the results of m -transformation. With high-pass filter sections R is the image impedance at the frequency $\nu = \infty$, and for band-pass filter sections that at the frequency $\nu = \nu_0$, the resonance frequency of the two branches Z_1 and Z_2 . This frequency ν_0 is the mean proportion between the two limiting frequencies ν_1 and ν_2 and also at the same time the mean proportion of the two frequencies with infinite attenuation $\nu_{1\infty}$ and $\nu_{2\infty}$.

One of these frequencies with infinite attenuation can be chosen arbitrarily, and then determines the other frequency with infinite attenuation which lies in the other attenuation band, as well as the parameter m . In the following section (double m -transformation) we will however encounter band-pass filter sections, in which the two frequencies with infinite attenuation can be arbitrarily chosen independent of each other.

As in the case of the low-pass filter sections, so also with the high-pass and band-pass filter sections, Z_T in the m_π -transformation and Z_π in the m_T -transformation are comparatively constant throughout the transmission band, if m is made about 0.6 (see fig. 13 in the previous article). Thus as a rule, here also, half-sections with m equal to approx. 0.6 can be chosen as terminal half-sections in a compound filter.

When $Z_1/4 Z_2$ has been determined for one filter section, then figs. 19, 20 and 21 can be employed to derive the attenuation constant α and the phase constant β by the method discussed in the previous article for low-pass filter sections.

How a T -section, a Π -section and a half-section are derived from the full branches given in the tables and how a compound filter can be built up from these sections require no further elucidation here, in view of the full analysis already given for low-pass filters.

Double m -Transformations of Band-Pass Filter Sections

In addition to the m -transformations already discussed, other transformations can also be

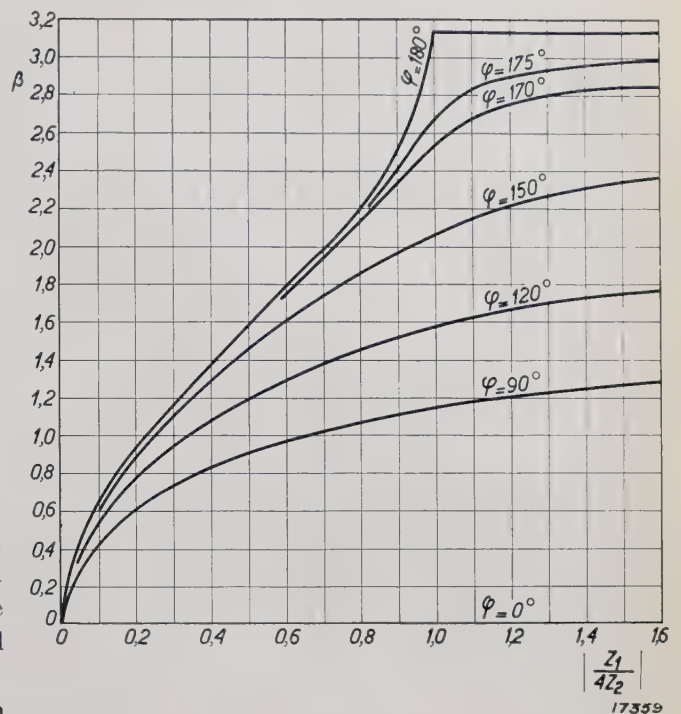


Fig. 21. Phase constant β (imaginary component of the propagation constant T) as a function of $|Z_1/4 Z_2|$ for T - and Π -sections.

performed with band-pass filters, which similarly permit other types of filter sections to be derived from the basic type, in which the limiting frequencies and one of the image impedances remain the same, while the other image impedance and the propagation constant T are different. In certain cases these transformations give sections of simpler construction, which are frequently employed for building up compound filters.

For the basic type we have found:

$$Z_1' = j \omega L_1' + \frac{1}{j \omega C_1'}$$

On m_T -transformation we get:

$$Z_1 = m Z_1' = j m \omega L_1' + \frac{m}{j \omega C_1'}$$

and Z_2 is defined such that $Z_T = \sqrt{Z_1 Z_2} \sqrt{1 + Z_1/4 Z_2}$ remains the same as for the basic type. But if we multiply L_1' by a positive, real number m_1 and divide C_1' by another positive, real number m_2 , we then get

$$Z_1 = j m_1 \omega L_1' + \frac{m_2}{j \omega C_1'}$$

If we now seek for a corresponding impedance Z_2 , such that $Z_T = Z_T'$, then these values of Z_1 and Z_2 represent the full branches of another filter section, whose Z_T is the same for all frequencies as that of the basic type. This signifies that the limiting

Tabel I

		Lowpass filter sections	Highpass filter sections	Bandpass filter sections
Basic type				
$Z_1' Z_2' = R^2$		$\frac{L_1'}{C_2'}$	$\frac{L_2'}{C_1'}$	$\sqrt{\frac{L_1' L_2'}{C_1' C_2'}}$
$\frac{Z_1'}{4 Z_2'}$	Without losses $d = 0$	$-x^2$	$-1/x^2$	$-y^2 = -\frac{(x-1/x)^2}{(x_2-x_1)^2}$
	With losses $d \neq 0$	$-x^2 (1-jd_L) (1-jd_C)$	$\frac{-1}{x^2 (1-jd_L) (1-jd_C)}$	$-\frac{1}{(x_2-x_1)^2} \cdot \frac{1-jd_C}{1-jd_L} \cdot \left[x (1-jd_L) - \frac{1}{x (1-jd_C)} \right]^2$
Transmission band $-1 < Z_1'/4 Z_2' < 0$		$0 < x < 1$	$1 < x < \infty$	$x_1 < x < x_2$
Infinite attenuation $ Z_1'/4 Z_2' = \infty$		$x_\infty = \infty$	$x_\infty = 0$	$x_{1\infty} = 0; x_{2\infty} = \infty$
$Z_T' = \sqrt{Z_1' Z_2'} \sqrt{1 + \frac{Z_1'}{4 Z_2'}}$		$R \sqrt{1-x^2}$	$R \sqrt{1-\frac{1}{x^2}}$	$R \sqrt{1-y^2}$
$Z_\pi' = \frac{\sqrt{Z_1' Z_2'}}{\sqrt{1 + Z_1'/4 Z_2'}}$		$\frac{R}{\sqrt{1-x^2}}$	$\frac{R}{\sqrt{1-1/x^2}}$	$\frac{R}{\sqrt{1-y^2}}$
m -transformations ($a = 1/\sqrt{1-m^2}$)				
$\frac{Z_1}{4 Z_2} = \frac{Z_1'}{4 Z_2'} \frac{m^2}{1 + \frac{1}{a^2} \frac{Z_1'}{4 Z_2'}}$		$\frac{a^2-1}{1-\frac{a^2}{x^2}}$	$\frac{a^2-1}{1-a^2 x^2}$	$\frac{a^2-1}{1-\frac{a^2}{y^2}}$
Transmission band		As basic type	As basic type	As basic type
Infinite attenuation $Z_1'/4 Z_2' = -a^2$		$x_\infty = a$	$x_\infty = \frac{1}{a}$	$y_\infty = \pm a$ $x_{2\infty} - x_{1\infty} = a (x_2 - x_1)$ $x_{1\infty} x_{2\infty} = 1$
m_T -transformation				
$Z_T = Z_T'$		$R \sqrt{1-x^2}$	$R \sqrt{1-1/x^2}$	$R \sqrt{1-y^2}$
$Z_\pi = Z_\pi' \left(1 + \frac{1}{a^2} \frac{Z_1'}{4 Z_2'} \right)$		$R \frac{1-\frac{x^2}{a^2}}{\sqrt{1-x^2}}$	$R \frac{1-\frac{1}{a^2 x^2}}{\sqrt{1-1/x^2}}$	$R \frac{1-\frac{y^2}{a^2}}{\sqrt{1-y^2}}$
m_π -transformation				
$Z_T = Z_T' \frac{1}{1 + \frac{1}{a^2} \frac{Z_1'}{4 Z_2'}}$		$R \frac{\sqrt{1-x^2}}{1-\frac{x^2}{a^2}}$	$R \frac{\sqrt{1-1/x^2}}{1-\frac{1}{a^2 x^2}}$	$R \frac{\sqrt{1-y^2}}{1-\frac{y^2}{a^2}}$
$Z_\pi = Z_\pi'$		$\frac{R}{\sqrt{1-x^2}}$	$\frac{R}{\sqrt{1-1/x^2}}$	$\frac{R}{\sqrt{1-y^2}}$
Definitions		$x = \frac{v}{v_1};$ $2 \pi v_1 = \frac{2}{\sqrt{L_1' C_2'}}$	$x = \frac{v}{v_1};$ $2 \pi v_1 = \frac{1}{2 \sqrt{L_2' C_1'}}$	$x_1 x_2 = 1; x_2 - x_1 = 2 \sqrt{\frac{L_2' C_1'}{L_1' C_2'}};$ $x = \frac{v}{v_0}; 2 \pi v_0 = \frac{1}{\sqrt{L_1' L_2' C_1' C_2'}}$

frequencies are also unchanged; for on exceeding the limiting frequencies, the image impedances change from a real to an imaginary value and *vice versa*. Calculation shows that this impedance Z_2 is of the form shown in fig. 22; in this figure the values of the components are also given. It can also be substituted by the equivalent circuit shown in Table II; Band-pass filter sections II_1 . Usually the latter circuit will be given preference, since the values of the self-inductances and the condensers are then as a rule neither too large nor too small, as might frequently happen with the circuit shown in fig. 22. Yet to derive still further filter sections we will for the sake of simplicity employ the circuit shown in fig. 22.

The impedance Z_2 can only be realised when m_1 and m_2 satisfy the following conditions:

$0 < m_1 < 1;$

$0 < m_2 < 1;$

$\frac{x_2}{x_1} \geq \frac{m_1}{m_2} \geq \frac{x_1}{x_2}.$

}

The sections obtained by “double m -transformation” are composed of the same L ’s and C ’s as the

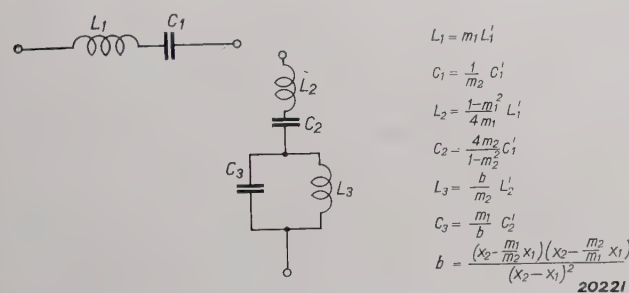


Fig. 22. Full branches of a band pass filter obtained by double m -transformation from the basic type. L_1' , L_2' , C_1' , C_2' are the values of the components for the basic type, and x_1 and x_2 are the limiting frequencies (see Table II, column I_1).

band-pass filter sections I_2 obtained by simple m -transformation, although $x = 1$ is now no longer valid for the resonance frequencies of the two branches and the two frequencies with infinite attenuation $x_{1\infty}$ and $x_{2\infty}$ are no longer inter-related by the equation $x_{1\infty} \cdot x_{2\infty} = 1$. By a suitable value of m_1 and m_2 , $x_{1\infty}$ and $x_{2\infty}$ can be arbitrarily chosen independent of each other, provided a frequency with infinite attenuation is located in each attenuation band.

A double m -transformation may be performed on exactly the same lines on the basic type in such a manner that Z_π remains equal to Z_π' of the basic type.

In Table II: Band-pass filter sections, II , the circuits for the full branches after double m_T and

double m_π transformations are given, as well as the values of the components. L_1' , C_1' , L_2' and C_2' are the values of the elements of the basic type (see column I_1). If the limiting frequencies x_1 and x_2 , the frequencies with infinite attenuation $x_{1\infty}$ and $x_{2\infty}$ and the image impedance R for the frequency $x = 1$ are given, as is usually the case in practice, the values of the components can be calculated. The propagation constant $T = \alpha + i\beta$ for these sections is most easily calculated by adding the propagation constants of two simpler types of section, which have still to be analysed, as indicated in Table II. The qualitative variation of α and β as a function of the frequency is similar to that found with the single m -transformation.

Special Cases of Double m -Transformation. Simpler Sections.

For certain values of m_1 and m_2 the sections assume a simpler form; these special cases are summarised in Table III.

The following special cases are differentiated in the double m_T -transformation.

	The twofold m -transformation passes over into single m -transformation. The filter section corresponds to type	II_1
$m_1 = m_2 \neq 1$	The fundamental type is obtained	I_1
$m_1 = m_2 = 1$	In fig. 22, C_2 becomes infinity, and a filter section is obtained aequivalent with type	V_1
$m_1 \neq 1, m_2 = 1$	In fig. 22, C_2 becomes zero, and a filter section is obtained aequivalent with type	V_2
$m_1 = 1, m_2 \neq 1$	In fig. 22, b becomes zero, from which follows: $L_3 = 0$, $C_3 = \infty$, and a filter section is obtained of type	IV_1
$\frac{m_1}{m_2} = \frac{x_2}{x_1}$	Similarly $b = 0$, $L_3 = 0$ and $C_3 = \infty$; and a filter section is obtained of type	IV_2
$\frac{m_1}{m_2} = \frac{x_1}{x_2}$	In fig. 22, $L_3 = 0$, $C_3 = \infty$, $L_2 = 0$, and a filter section is obtained of type	III_1
$m_1 = 1, m_2 = \frac{x_1}{x_2}$	In fig. 22 $L_3 = 0$, $C_3 = \infty$, $C_2 = \infty$, and a filter section is obtained of type	III_2

The same eight special cases occur under the same conditions in the double m_π -transformation, for which the relevant formulae and the data are also given in Table III. Sections after m_T -transforma-

tion are only used in the T form and those after m_π -transformation only in the II form, as otherwise it is not possible to connect up separate sections of a compound filter with equal image impedances side by side. No formulae are given in the figures for those image impedances having no direct bearing on such compounding, but only qualitative curves, whose irregular shape in the transmission band is already sufficient indication of their unsuitability and of the need for avoiding them.

For the sections of types II and V the propagation constant $T = \alpha + i\beta$ is best determined not by calculating $Z_1/4 Z_2$, but by addition of the values of α and β for two simpler sections, which are given in the Table II and III for each section of type II or V . The propagation constants of the simpler sections are calculated by substituting in the indicated formulae those values of $x_{l\infty}$ and $x_{2\infty}$ which are employed for the sections of type II or V under consideration. Thus for type II the sections IV_1 and IV_2 are indicated, and in order to determine α for these filter sections $Z_1/4 Z_2$ is first calculated for the IV_1 section with that value of $x_{2\infty}$ as employed in II , then deriving the corresponding attenuation coefficient α from fig. 19 or 20. This is followed by the calculation of $Z_1/4 Z_2$ for section IV_2 with the same value of $x_{l\infty}$ as given for the type II section, again reading the corresponding value of α from fig. 19 or 20, and finally adding the two attenuation values of α so obtained. The imaginary term β of the propagation constant is derived in exactly the same way with the aid of fig. 21.

If a thorough grasp has been obtained of the theory of electrical filters outlined in this series of articles, the data given in Tables II and III and in figs. 19, 20 and 21 will be found sufficient for evolving any filter to meet specific requirements included among the usual types employed in practice. This may be suitably demonstrated by a specific example.

Example

It is required to design a low-pass filter to meet the following requirements: The filter is to be used in the anode circuit of a triode with an internal resistance of 10 000 ohms. With a constant alternating voltage applied to the grid of the triode, the secondary voltage of the filter must not vary more than 1 decibel from a specific mean value for frequencies below 900 cycles/sec (the voltage must therefore be maintained between 0.89 and 1.12 per cent of this mean value), and for frequencies above 1100 cycles/sec it must be less than 1/500 of this mean

value. The attenuation must therefore be at least 54 decibels. The losses in the coils, which it is proposed to use, at frequencies above 1000 cycles/sec, and those of the condensers throughout the whole frequency sweep have such values that $r/\omega L = R/\omega C = 0.02$. It is further assumed that the losses in the coils below 1000 cycles/sec are exclusively due to a D.C. resistance, and are thus independent of the frequency. Then for $\nu > 1000$ cycles/sec, $d_L = d_C = 0.02$; for $\nu < 1000$ cycles/sec, $d_L = 0.02 \cdot 1000/\nu$.

No conditions are laid down for the frequency band between 900 and 1100 cycles/sec; this is therefore the transition range between the transmission and the attenuation bands. The limiting frequency ν_1 is taken in the middle of this band, so that $\nu_1 = 1000$ cycles/sec.

Firstly, the type and number of the filter sections required are determined; this is followed by the determination of the ratings of the filter components. In the transmission band required ($\nu = 0$ to 900 cycles, i.e. $x < 0.9$), the attenuation must be adequately constant. To satisfy this condition

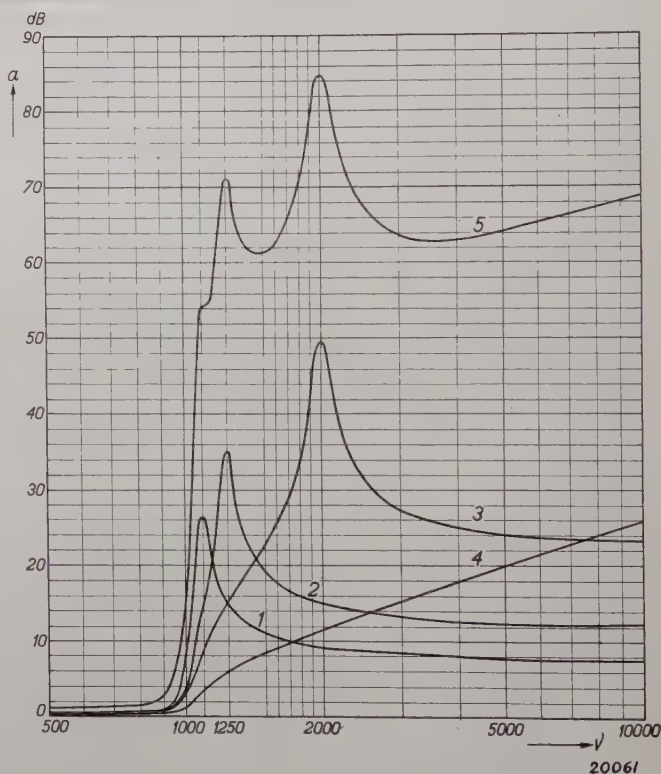


Fig. 23. Attenuation constant α of a low-pass filter composed of four sections, plotted as a function of the frequency.

1. Attenuation of a section with $x_\infty = 1.1$.
2. Attenuation of both terminal half-sections with $m = 0.6$ ($x_\infty = 1.25$), which together may be regarded as a single section.
3. Attenuation of a section with $x_\infty = 2.0$.
4. Attenuation of a half-section of the basic type.
5. Total attenuation.

LOW PASS FILTER SECTIONS				HIGH PASS FILTER SECTIONS			BAND PASS FILTER SECTIONS I			BAND PASS FILTER SECTIONS II	
TYPE NUMBER	1	2	3	1	2	3	I ₁	I ₂	I ₃	II ₁	II ₂
FULL BRANCHES	BASIC TYPE	m _T -TRANSFORMATION	m _π -TRANSFORMATION	BASIC TYPE	m _T -TRANSFORMATION	m _π -TRANSFORMATION	BASIC TYPE	m _T -TRANSFORMATION	m _π -TRANSFORMATION	DOUBLE m _T -TRANSFORMATION	DOUBLE m _π -TRANSFORMATION
VALUES OF THE ELEMENTS	$L_1' = \frac{R}{\pi \nu_1}$ $C_2' = \frac{1}{\pi \nu_1 R}$	$L_1 = m L_1'$ $L_2 = \frac{1-m^2}{4m} L_1'$ $C_2 = m C_2'$	$L_1 = m L_1'$ $C_1 = \frac{1-m^2}{4m} C_2'$ $C_2 = m C_2'$	$C_1' = \frac{1}{4\pi \nu_1 R}$ $L_2' = \frac{R}{4\pi \nu_1}$	$C_1 = \frac{C_1'}{m}$ $C_2 = \frac{4m}{1-m^2} C_1'$ $L_2 = \frac{L_2'}{m}$	$C_1 = \frac{C_1'}{m}$ $L_1 = \frac{4m}{1-m^2} L_2'$ $L_2 = \frac{L_2'}{m}$	$L_1' = \frac{R}{\pi \nu_0 (x_2 - x_1)}$ $C_1' = \frac{x_2 - x_1}{4\pi \nu_0 R}$ $L_2' = \frac{(x_2 - x_1) R}{4\pi \nu_0}$ $C_2' = \frac{1}{\pi \nu_0 (x_2 - x_1) R}$	$L_1 = m L_1'$ $C_1 = \frac{1}{m} C_1'$ $L_2 = \frac{1-m^2}{4m} (1+x_{1\infty}^2) L_1'$ $C_2 = \frac{4m}{1-m^2} \frac{1}{1+x_{2\infty}^2} C_1'$ $L_3 = \frac{1-m^2}{4m} (1+x_{2\infty}^2) L_1'$ $C_3 = \frac{4m}{1-m^2} \frac{1}{1+x_{1\infty}^2} C_1'$	$L_1 = \frac{4m}{1-m^2} \frac{1}{1+x_{2\infty}^2} L_2'$ $C_1 = \frac{1-m^2}{4m} (1+x_{1\infty}^2) C_2'$ $L_2 = \frac{1-m^2}{4m} \frac{1}{1+x_{1\infty}^2} L_2'$ $C_2 = \frac{1-m^2}{4m} (1+x_{2\infty}^2) C_2'$ $L_3 = \frac{1}{m} L_2'$ $C_3 = m C_2'$	$L_1 = m_1 L_1'$ $C_1 = \frac{1}{m_2} C_1'$ $L_2 = a L_1'$ $C_2 = \frac{1}{b} C_1'$ $L_3 = c L_1'$ $C_3 = \frac{1}{d} C_1'$	$L_1 = \frac{1}{b} L_2'$ $C_1 = a C_2'$ $L_2 = \frac{1}{d} L_2'$ $C_2 = c C_2'$ $L_3 = \frac{1}{m_2} L_2'$ $C_3 = m_1 C_2'$
$Z_T = \sqrt{Z_1 Z_2} \sqrt{1 + \frac{Z_1}{4Z_2}}$											
$Z_T' = R \sqrt{1-x^2}$	$Z_T' = R \sqrt{1-x^2}$	$Z_T' = R \sqrt{1-x^2}$	$Z_T' = R \sqrt{1-x^2}$	$Z_T' = R \sqrt{1-x^2}$	$Z_T' = R \sqrt{1-x^2}$	$Z_T' = R \sqrt{1-x^2}$	$Z_T' = R \sqrt{1-y^2}$	$Z_T' = R \sqrt{1-y^2}$	$Z_T' = R \sqrt{1-y^2}$	$Z_T' = R \sqrt{1-y^2}$	$Z_T' = R \sqrt{1-y^2}$
$Z_{\pi} = \frac{\sqrt{Z_1 Z_2}}{\sqrt{1 + \frac{Z_1}{4Z_2}}}$											
$Z_{\pi}' = \frac{R}{\sqrt{1-x^2}}$	$Z_{\pi}' = \frac{R}{\sqrt{1-x^2}}$	$Z_{\pi}' = \frac{R}{\sqrt{1-x^2}}$	$Z_{\pi}' = \frac{R}{\sqrt{1-x^2}}$	$Z_{\pi}' = \frac{R}{\sqrt{1-x^2}}$	$Z_{\pi}' = \frac{R}{\sqrt{1-x^2}}$	$Z_{\pi}' = \frac{R}{\sqrt{1-x^2}}$	$Z_{\pi}' = \frac{R}{\sqrt{1-y^2}}$	$Z_{\pi}' = \frac{R}{\sqrt{1-y^2}}$	$Z_{\pi}' = \frac{R}{\sqrt{1-y^2}}$	$Z_{\pi}' = \frac{R}{\sqrt{1-y^2}}$	$Z_{\pi}' = \frac{R}{\sqrt{1-y^2}}$
ATTENUATION CONSTANT α FOR ELEMENTS WITHOUT LOSSES											
PHASE CONSTANT β FOR ELEMENTS WITHOUT LOSSES											
$\frac{Z_1}{4Z_2}$	WITHOUT LOSSES $d=0$ $-x^2$ WITH LOSSES $d \neq 0$ $-x^2(1-jd_c)(1-jd_c)$	$\frac{a^2-1}{1-a^2x^2}$ $\frac{a^2-1}{1-x^2(1-jd_c)(1-jd_c)}$	$\frac{a^2-1}{1-a^2x^2}$ $\frac{a^2-1}{1-x^2(1-jd_c)(1-jd_c)}$	$-\frac{1}{x^2}$ $-\frac{1}{x^2(1-jd_c)(1-jd_c)}$	$\frac{a^2-1}{1-a^2x^2}$ $\frac{a^2-1}{1-x^2(1-jd_c)(1-jd_c)}$	$\frac{a^2-1}{1-a^2x^2}$ $\frac{a^2-1}{1-x^2(1-jd_c)(1-jd_c)}$	$-y^2$ y^2 REPLACE BY $\frac{1}{(x_2-x_1)^2} \frac{1-jd_c}{1-jd_c} \left[x(1-jd_c) - \frac{1}{x(1-jd_c)} \right]^2$	$-\frac{a^2-1}{1-y^2}$ $\frac{a^2-1}{1-y^2}$	$-\frac{a^2-1}{1-y^2}$ $\frac{a^2-1}{1-y^2}$	$T = \alpha + j\beta$ IS THE SUM OF THE T'S OF TYPES II ₁ AND II ₂ WITH THE SAME VALUES x_{∞} AND $x_{1\infty}$ RESPECTIVELY	$T = \alpha + j\beta$ IS THE SUM OF THE T'S OF TYPES II ₁ AND II ₂ WITH THE SAME VALUES x_{∞} AND $x_{1\infty}$ RESPECTIVELY
DEFINITIONS	$x = \frac{\nu}{\nu_1}$ $x_{\infty} = \frac{\nu_{\infty}}{\nu_1} = a$	$m^2 = 1 - \frac{1}{a^2}$ $a^2 = \frac{1}{1-m^2}$	$d_c = \frac{r_c}{\omega L}$ $d_c = \frac{1}{R_c \omega C}$	$x = \frac{\nu}{\nu_1}$ $x_{\infty} = \frac{\nu_{\infty}}{\nu_1} = \frac{1}{a}$	$m^2 = 1 - \frac{1}{a^2}$ $a^2 = \frac{1}{1-m^2}$	$d_c = \frac{r_c}{\omega L}$ $d_c = \frac{1}{R_c \omega C}$	$\nu_0^2 = \nu_1 \nu_2 = \nu_{1\infty} \nu_{2\infty}$ $x_1 x_2 = x_{1\infty} x_{2\infty} = 1$ $m^2 = 1 - \frac{1}{a^2}$ $a^2 = \frac{1}{1-m^2}$ $d_c = \frac{1}{R_c \omega C}$	$\nu_0^2 = \nu_1 \nu_2$ $x_1 x_2 = 1$ $m_1 = \frac{g}{x_{2\infty} + h}$ $m_2 = \frac{g+h x_{1\infty}}{1-x_{2\infty}^2}$ $y = \frac{x-1}{x_2-x_1}$ $g = \sqrt{(x_1^2-x_{1\infty}^2)(x_2^2-x_{2\infty}^2)}$ $h = \sqrt{(1-x_{2\infty}^2)(1-x_{1\infty}^2)}$	$\nu_0^2 = \nu_1 \nu_2$ $x_1 x_2 = 1$ $m_1 = \frac{g}{x_{2\infty} + h}$ $m_2 = \frac{g+h x_{1\infty}}{1-x_{2\infty}^2}$ $y = \frac{x-1}{x_2-x_1}$ $g = \sqrt{(x_1^2-x_{1\infty}^2)(x_2^2-x_{2\infty}^2)}$ $h = \sqrt{(1-x_{2\infty}^2)(1-x_{1\infty}^2)}$	$a = \frac{1-m^2}{4g} x_{2\infty}^2 (1 - \frac{x_{1\infty}}{x_{2\infty}})$ $b = \frac{1-m^2}{4g} (1 - \frac{x_{1\infty}}{x_{2\infty}})$ $c = \frac{1-m^2}{4g} (1 - \frac{x_{2\infty}}{x_{1\infty}})$ $d = \frac{1-m^2}{4h} x_{2\infty}^2 (1 - \frac{x_{1\infty}}{x_{2\infty}})$	$a = \frac{1-m^2}{4g} x_{2\infty}^2 (1 - \frac{x_{1\infty}}{x_{2\infty}})$ $b = \frac{1-m^2}{4g} (1 - \frac{x_{1\infty}}{x_{2\infty}})$ $c = \frac{1-m^2}{4g} (1 - \frac{x_{2\infty}}{x_{1\infty}})$ $d = \frac{1-m^2}{4h} x_{2\infty}^2 (1 - \frac{x_{1\infty}}{x_{2\infty}})$

Table II. Data for the designs of low-pass, high-pass and band-pass filters.

		BAND PASS FILTER SECTIONS III				BAND PASS FILTER SECTIONS IV				BAND PASS FILTER SECTIONS V				
TYPE NUMBER		III ₁	III ₂	III ₃	III ₄	IV ₁	IV ₂	IV ₃	IV ₄	V ₁	V ₂	V ₃	V ₄	
FULL BRANCHES		m_T - TRANSFORMATION		m_{TT} - TRANSFORMATION		m_T - TRANSFORMATION		m_{TT} - TRANSFORMATION		m_T - TRANSFORMATION		m_{TT} - TRANSFORMATION		
VALUES OF THE ELEMENTS		$L_1 = \frac{R}{\pi v_0(x_2 - x_1)} L_1'$ $C_1 = \frac{x_2 - x_1}{4\pi v_0 x_1^2 R}$ $C_2 = \frac{1}{\pi v_0(x_1 + x_2)R}$	$L_1 = \frac{x_1^2 R}{\pi v_0(x_2 - x_1)}$ $C_1 = \frac{x_2 - x_1}{4\pi v_0 x_1^2 R}$ $L_2 = \frac{(x_1 + x_2) R}{4\pi v_0}$	$L_1 = \frac{R}{\pi v_0(x_1 + x_2)}$ $L_2 = \frac{(x_2 - x_1) R}{4\pi v_0 x_1^2}$ $C_2 = \frac{1}{\pi v_0(x_2 - x_1)R}$	$C_1 = \frac{x_1 + x_2}{4\pi v_0 R}$ $L_2 = \frac{(x_2 - x_1) R}{4\pi v_0 x_1^2}$ $C_2 = \frac{x_1^2}{\pi v_0(x_2 - x_1)R}$	$L_1 = m_1 L_1'$ $C_1 = \frac{1}{m_1^2} C_1'$ $L_2 = \frac{1 - m_1^2}{4m_1} L_1'$ $C_2 = \frac{4m_1^2}{1 - m_1^2} C_1'$ $m_1 = \sqrt{\frac{x_2^2 - x_1^2}{x_2^2 - x_{1m}^2}}$ $m_2 = x_1^2 m_1$	$L_1 = m_1 L_1'$ $C_1 = \frac{1}{m_1^2} C_1'$ $L_2 = \frac{1 - m_1^2}{4m_1} L_1'$ $C_2 = \frac{4m_1^2}{1 - m_1^2} C_1'$ $m_1 = \sqrt{\frac{x_2^2 - x_1^2}{x_2^2 - x_{1m}^2}}$ $m_2 = x_1^2 m_1$	$L_1 = \frac{4m_2}{1 - m_2^2} L_2'$ $C_1 = \frac{1 - m_2^2}{4m_1} C_2'$ $L_2 = \frac{1}{m_2} L_2'$ $C_2 = m_1 C_2'$ $m_1 = \sqrt{\frac{x_2^2 - x_1^2}{x_2^2 - x_{1m}^2}}$ $m_2 = x_1^2 m_1$	$L_1 = \frac{4m_2}{1 - m_2^2} L_2'$ $C_1 = \frac{1 - m_2^2}{4m_1} C_2'$ $L_2 = \frac{1}{m_2} L_2'$ $C_2 = m_1 C_2'$ $m_1 = \sqrt{\frac{x_2^2 - x_1^2}{x_2^2 - x_{1m}^2}}$ $m_2 = x_1^2 m_1$	$L_1 = m_1 L_1'$ $C_1 = C_1'$ $L_2 = p L_1'$ $L_3 = \frac{1 - m^2}{4h} L_1'$ $C_3 = \frac{h}{p} C_1'$	$L_1 = L_1'$ $C_1 = \frac{1}{m_1^2} C_1'$ $L_2 = \frac{q}{g} L_1'$ $C_2 = \frac{4g}{1 - m_1^2} C_1'$ $C_3 = \frac{1}{q} C_1'$	$L_1 = \frac{h}{p} L_1'$ $C_1 = \frac{1 - m}{4h} C_1'$ $C_2 = p C_1'$ $L_3 = L_1'$ $C_3 = m C_1'$	$L_1 = \frac{4g}{1 - m} L_1'$ $C_1 = \frac{q}{g} C_1'$ $L_2 = \frac{1}{q} L_1'$ $L_3 = \frac{1}{m} L_1'$ $C_3 = C_2'$	
$Z_T = \sqrt{Z_1 Z_2} \sqrt{1 + \frac{Z_1}{4Z_2}}$														
$Z_T = R \sqrt{1 - y^2} (= Z_T')$		$Z_T = R \sqrt{1 - y^2} (= Z_T')$	$Z_T = R \sqrt{1 - y^2} (= Z_T')$	$Z_T = R \sqrt{1 - y^2} (= Z_T')$	$Z_T = R \sqrt{1 - y^2} (= Z_T')$	$Z_T = R \sqrt{1 - y^2} (= Z_T')$	$Z_T = R \sqrt{1 - y^2} (= Z_T')$	$Z_T = R \sqrt{1 - y^2} (= Z_T')$	$Z_T = R \sqrt{1 - y^2} (= Z_T')$	$Z_T = R \sqrt{1 - y^2} (= Z_T')$	$Z_T = R \sqrt{1 - y^2} (= Z_T')$	$Z_T = R \sqrt{1 - y^2} (= Z_T')$	$Z_T = R \sqrt{1 - y^2} (= Z_T')$	
$Z_T = \frac{\sqrt{Z_1 Z_2}}{\sqrt{1 + \frac{Z_1}{4Z_2}}}$														
$Z_T = \frac{R}{\sqrt{1 - y^2}} (= Z_T')$		$Z_T = \frac{R}{\sqrt{1 - y^2}} (= Z_T')$	$Z_T = \frac{R}{\sqrt{1 - y^2}} (= Z_T')$	$Z_T = \frac{R}{\sqrt{1 - y^2}} (= Z_T')$	$Z_T = \frac{R}{\sqrt{1 - y^2}} (= Z_T')$	$Z_T = \frac{R}{\sqrt{1 - y^2}} (= Z_T')$	$Z_T = \frac{R}{\sqrt{1 - y^2}} (= Z_T')$	$Z_T = \frac{R}{\sqrt{1 - y^2}} (= Z_T')$	$Z_T = \frac{R}{\sqrt{1 - y^2}} (= Z_T')$	$Z_T = \frac{R}{\sqrt{1 - y^2}} (= Z_T')$	$Z_T = \frac{R}{\sqrt{1 - y^2}} (= Z_T')$	$Z_T = \frac{R}{\sqrt{1 - y^2}} (= Z_T')$	$Z_T = \frac{R}{\sqrt{1 - y^2}} (= Z_T')$	
ATTENUATION CONSTANT α FOR ELEMENTS WITHOUT LOSSES														
PHASE CONSTANT β FOR ELEMENTS WITHOUT LOSSES														
$T = \alpha + j\beta$ IS THE SUM OF THE T'S OF TYPES LISTED BELOW WITH THE SAME VALUES x_{1m} and x_{2m}		x^2 REPLACE BY $x^2 (1 - j d_c) (1 - j d_c)$				x^2 REPLACE BY $x^2 (1 - j d_c) (1 - j d_c)$				$T = \alpha + j\beta$ IS THE SUM OF THE T'S OF TYPES LISTED BELOW WITH THE SAME VALUES x_{1m} and x_{2m}				
Z_1, Z_2		WITHOUT LOSSES $d=0$ $\frac{x_1^2 - x^2}{x_2^2 - x_1^2}$	$\frac{x_1^2 - x^2}{x_2^2 - x_1^2}$	$\frac{x_1^2 - x^2}{x_2^2 - x_1^2}$	$\frac{x_1^2 - x^2}{x_2^2 - x_1^2}$	$\frac{(x_2^2 - x_{1m}^2)(x^2 - x_1^2)}{(x_2^2 - x_1^2)(x_{2m}^2 - x^2)}$	$\frac{(x_1^2 - x_1^2)(x^2 - x_2^2)}{(x_1^2 - x_2^2)(x_{1m}^2 - x^2)}$	$\frac{(x_2^2 - x_{1m}^2)(x^2 - x_1^2)}{(x_2^2 - x_1^2)(x_{2m}^2 - x^2)}$	$\frac{(x_1^2 - x_1^2)(x^2 - x_2^2)}{(x_1^2 - x_2^2)(x_{1m}^2 - x^2)}$	$T = \alpha + j\beta$ IS THE SUM OF THE T'S OF TYPES LISTED BELOW WITH THE SAME VALUES x_{1m} and x_{2m}				
WITH LOSSES $d \neq 0$		x^2 REPLACE BY $x^2 (1 - j d_c) (1 - j d_c)$				x^2 REPLACE BY $x^2 (1 - j d_c) (1 - j d_c)$				$T = \alpha + j\beta$ IS THE SUM OF THE T'S OF TYPES LISTED BELOW WITH THE SAME VALUES x_{1m} and x_{2m}				
DEFINITIONS		$v_0^2 = v_1 v_2$ $x = \frac{v}{v_0}$	$x_1 = \frac{v_1}{v_0}$ $x_2 = \frac{v_2}{v_0}$	$y = \frac{x - \frac{1}{x}}{x_2 - x_1}$ $x_1, x_2 = 1$	$d_c = \frac{r_L}{\omega L}$ $d_c = \frac{1}{R_c \omega C}$	$v_0^2 = v_1 v_2$ $x = \frac{v}{v_0}$	$x_1 = \frac{v_1}{v_0}$ $x_2 = \frac{v_2}{v_0}$	$x_{1m} = \frac{v_{1m}}{v_0}$ $x_{2m} = \frac{v_{2m}}{v_0}$	$y = \frac{x - \frac{1}{x}}{x_2 - x_1}$ $x_1, x_2 = 1$	$d_c = \frac{r_L}{\omega L}$ $d_c = \frac{1}{R_c \omega C}$	$v_0^2 = v_1 v_2$ $x = \frac{v}{v_0}$	$x_{1m} = \frac{v_{1m}}{v_0}$ $x_{2m} = \frac{v_{2m}}{v_0}$	$g = \sqrt{(x_1^2 - x_{1m}^2)(x_2^2 - x_{2m}^2)}$ $h = \sqrt{\left(\frac{1}{x_1^2} - \frac{1}{x_2^2}\right)\left(\frac{1}{x_2^2} - \frac{1}{x_{2m}^2}\right)}$ $m_1 = \frac{1}{x_2^2} + h$ $m_2 = x_{1m}^2 + g$	$p = \frac{1 - m_1^2}{4} x_{2m}^2$ $q = \frac{1 - m_2^2}{4} x_{1m}^2$

the supplementary attenuation produced at the two terminals of the filter by the deviation of the image impedances from the terminating resistances must be small. As already indicated on p. 302, this may be achieved by terminating the filter at both ends with half-sections obtained by m -transformation, where $m = 0.6$. The image impedances of the whole filter, which are equal to the image impedances of the terminating sections, are then nearly constant for $x < 0.9$, and to a first approximation the supplementary attenuation just referred to can be neglected. Since this conforms with the most common practical case, the calculation of the supplementary attenuation will be omitted here in order to simplify the analysis. The two half-sections together give the same attenuation as a whole section. If the attenuation of this section is calculated for a number of frequencies, the attenuation curve 2 in fig. 23 is obtained. The "frequency with infinite attenuation" (for which, as already shown in a previous article, the attenuation with a dissipative filter is not really infinite but has a maximum value) is $x_\infty = a = 1/\sqrt{1-m^2} = 1.25$. For frequencies in the neighbourhood of the frequency with infinite attenuation ($x = 1.25$) and close to the limiting frequency (but $x > 1$), the value of $Z_1/4Z_2$ including into consideration the losses may be obtained from the expression:

$$\begin{aligned} \frac{Z_1}{4Z_2} &= \frac{a^2 - 1}{1 - \frac{a^2}{x^2(1-jd_L)(1-jd_C)}} = \\ &= \frac{0.5625}{1 - \frac{1.5625}{x^2(1-j0.04)}} \end{aligned}$$

(At $x < 1$ we must insert a higher value for d_L , viz., $0.02/x$.) For the remaining frequencies (in the present case for $x \geq 1.5$) the effect of the losses in the filter components can be neglected and the following simplified equation found applicable to a sufficient degree of approximation:

$$\frac{Z_1}{4Z_2} = \frac{a^2 - 1}{1 - \frac{a^2}{x^2}} = \frac{0.5625}{1 - \frac{1.5625}{x^2}}$$

As an example, we calculate the attenuation constant of the section under consideration for $x = 1.2$:

$$\frac{Z_1}{4Z_2} = \frac{0.5625}{1 - \frac{1.5625}{1.44(1-j0.04)}} = -5.31 + j \cdot 2.76.$$

From this it follows:

$$\begin{aligned} \left| \frac{Z_1}{4Z_2} \right| &= \sqrt{5.31^2 + 2.76^2} = 5.98; \\ \operatorname{tg} \varphi &= -\frac{2.76}{5.31} = 0.520; \\ \varphi &= 152^\circ 30'. \end{aligned}$$

From fig. 20 we then get for this frequency: $a = 28$ decibels.

We must now investigate which forms of sections can be inserted between these two half-sections in order to satisfy the requirements as regards attenuation. The lowest frequency for which a given attenuation is stipulated is $x = 1.1$, which is fairly close to the limiting frequency. To obtain adequate attenuation at this frequency a section with $x_\infty = a = 1.1$ must be used, since sections with higher values of a give too low an attenuation so close to the limiting frequency. Exactly as for the terminal sections with $a = 1.25$ ($m = 0.6$), the attenuation curve is deduced for this section (fig. 23, curve 1). It is found that both sections together give an attenuation of only 41 decibels at $x = 1.1$, which is thus not enough. Apart from the consideration of other points, further sections must therefore be added, which for $x = 1.1$ all add something to the attenuation. We must then examine whether the attenuation of the complete filter is adequate at $x = 1.1$.

It follows from curves 1 and 2 that the attenuation is still too low at $x > 1.5$. We therefore add a section with $x = a = 2$. The choice of this value of x_∞ is to some arbitrary, but with some experience in the construction of filters a reasonable close approximation to the correct value of x_∞ can be readily made. For this section we again calculate the attenuation curve (fig. 23, curve 3). On plotting the attenuation curve for the three sections connected in series, which is equivalent to the sum of the attenuations of the separate sections, it is observed that the attenuation above $x > 2$ progressively diminishes with increasing frequency. To obtain adequate attenuation for $x > 3$, still another section must hence be added which will give a high attenuation particularly at high frequencies, e.g. a section of the basic type. The attenuation of a half-section of the basic type, i.e. half the attenuation of a whole section, is found to be already sufficient. The attenuation of this half-section is shown in curve 4 in fig. 23, while curve 5 gives the attenuation of the whole filter.

It now remains to be seen whether all conditions laid down at the outset have been fully met. In

the prescribed transmission band ($0 < x < 0.9$) the attenuation is between 1 and 3 decibels. The average is 2 decibels, and the attenuation does not vary from this by more than 1 decibel. The requirements as regards the transmission band have thus been met. In the required attenuation

slightly greater and is then adequate. Above $x > 2$ the attenuation is indeed reduced, but this is of no moment since the attenuation in this frequency band is even then more than enough. The values eventually arrived at in this analysis correspond to a filter with $x_\infty = a = 1.8$ for this section.

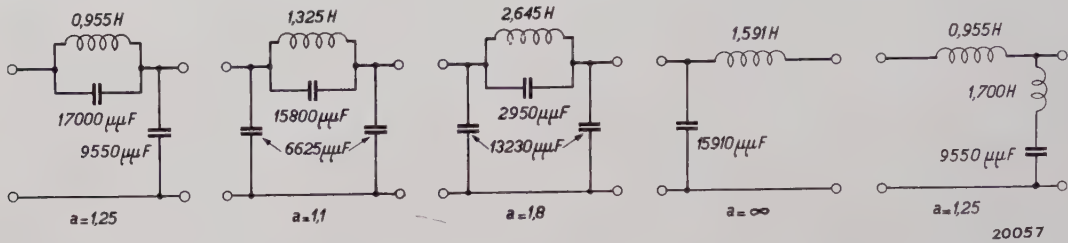


Fig. 24. Filter sections for a low-pass filter with a limiting frequency of 1000 cycles/sec. This filter satisfies the requirements set out on p. 336, if the coils and condensers have the ratings as stated there.

band ($x > 1.1$) the attenuation has to be $2 + 54 = 56$ decibels. We see that for $x = 1.1$ the attenuation is only 54 decibels; nevertheless this condition is adequately met for higher frequencies. In the majority of practical cases this difference of only 2 decibels is quite permissible (being moreover in a very narrow frequency range). In our case, however, there are several ways available for increasing the attenuation for $x = 1.1$. For instance, another filter section can be added, although this way out of the difficulty is rather expensive; also at the same time attenuation in the whole attenuation range becomes much greater than is necessary, and the filter becomes unnecessarily bulky and costly. A usually simpler solution consists in using a self-inductance of somewhat better quality, i.e. with a slightly lower value for $d_L = r/\omega L$ in the section with $a = 1.1$. As a result the attenuation for $x_\infty = a = 1.1$ is made much greater. But in the present case a still simpler solution can be adopted. For the section with $x_\infty = a = 2$ the value 2 was selected rather arbitrarily. If a is made 1.9 or 1.8, the attenuation of this section at $x = 1.1$ becomes

Finally, it must be decided whether the various sections are to be used in the T or the Π form. As regards attenuation these two forms are identical, only in the one case more coils are required and in the other more condensers. In general the circuit with the smaller number of coils is the less costly, so that if at all possible the Π type will be preferred here. Since, *inter alia*, a half-section of the fundamental type occurs, in which there is a spontaneous transition from Π sections to T sections, the one terminal half section will correspond to the m_T -transformation and the other to the m_π -transformation. We thus arrive at the sequence of sections shown in fig. 24. The numerical values indicated there for the components are calculated by the formulae in Table II by inserting $R = 10\,000$ ohms, and $\nu_l = 1000$ cycles/sec. If the individual sections are interconnected and the condensers in parallel are replaced by a single condenser equivalent to the sum of the two, and the self-inductances in series are also replaced by a single unit equivalent to the pair, then the filter shown in fig. 25 is obtained, which on the secondary side must be terminated by a resistance of 10 000 ohms.

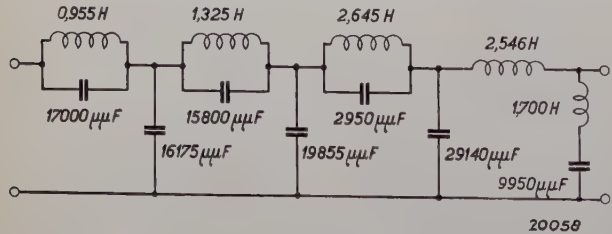


Fig. 25. Low-pass filter composed of the filter sections given in fig. 24.

The accuracy with which the self-inductances and condensers are calculated and calibrated must as a rule be so high that the ratings of the finished filter components do not differ more than 1 per cent from the theoretical values. Only for filters which have to satisfy particularly severe requirements is a higher degree of accuracy necessary.

SYSTEMATIC X-RAY EXAMINATION FOR THE DETECTION OF PULMONARY TUBERCULOSIS

By J. G. A. VAN WEEL.

Summary. A description is given of the application of X-ray screening as adopted by the medical welfare section of N.V. Philips for the detection of pulmonary tuberculosis. Examinations are made on all new entrants to the Works, the whole of the permanent staff, school-children and the families of patients suffering from pulmonary tuberculosis.

Introduction

The applications of X-rays in medical practice have steadily gained in importance during the last few decades, their progressive utilisation being due to the simultaneous development of theory and practice in two outstanding directions. Firstly, there has been the marked technological advance made in the construction of apparatus having a much greater range of application and affording both the patient and the radiologist better protection against the injurious action of the rays¹⁾ than hitherto. The other development is the recognition of the fact that in certain circumstances diagnosis cannot be based solely on the findings of ordinary clinical examination, and radiological examination is necessary to supplement clinical diagnosis. The omission to avail oneself of the advantages of a radiological examination is in many instances due to a lack of appreciation of its potentialities and value.

The aim of the radiological methods as an aid in diagnosis is to render visible the internal organs of the human body, either by radiography or by screening. Such examination can be based on either a natural contrast, (e.g. in pulmonary diagnosis) or on an artificial contrast as produced for the stomach, intestines and kidneys when using barium or other substance which has a marked absorption for X-rays.

A very important field of X-ray diagnosis lies in the examination of the thoracic cavity. Owing to the contained air the lungs produce a natural contrast with respect to surrounding organs, such as the heart and vascular system, and it is just this characteristic which can be used to advantage in the investigation of one of the most common

diseases of the thoracic cavity, viz., pulmonary tuberculosis.

It may be recalled that X-ray examination was originally employed to obtain a closer insight into the processes developing in the tubercular lung. At the present time it is also used for the active detection of tuberculosis. Pulmonary tuberculosis frequently develops without the patient at the outset complaining of any symptoms, and these cases of "unsuspected" tuberculosis can only be detected by systematic X-ray examination.

It would lead us too far to discuss fully all the advantages and disadvantages of the two methods employed for this purpose, viz., screening and radiography, and only the more important characteristics will be referred to.

The high cost of making radiographs is still the principal obstacle in the way of the general application of radiography for these investigations. Screening owing to its simple procedure and low cost is however eminently suitable for this purpose. One drawback of this method is that certain tubercular foci may escape detection. It would of course be far better if both methods could be applied simultaneously in all cases, but the high cost of radiography precludes this. The marked technical advances made have opened up a large field of application for screening, and large groups of persons can now be examined by screening almost at any place (offices, factories, schools, barracks, etc.), mainly owing to the construction of simple and portable screening equipment.

In a large industrial undertaking with a large staff, the active detection of tuberculosis among the employees enables early treatment to be given to those infected. Healthy persons, moreover, benefit by the reduced danger of infection when established cases of active tuberculosis are located in their early stages and given timely treatment.

A brief description is given here of the systematic X-ray examinations for the diagnosis of tuberculosis which are carried out in connection with the staff of the Philips Works at Eindhoven.

¹⁾ It should be noted in this connection that modern X-ray tubes, such as the Metalix, have been so thoroughly screened that no radiation is obtained outside the actual X-ray beam. It must not, however, be concluded from this that the radiologist is exposed to no danger at all provided he remains outside the beam, for although the primary beam has been adequately cut off the patient disperses rays which as a rule are of such intensity that in most cases additional precautions must be taken.

Procedure and Results

To combat resolutely the spread of pulmonary tuberculosis it is essential that every single individual is submitted to a proper examination; since tuberculosis is an infectious disease its origin must be sought among all persons (family, dependents, colleagues, apprentices, etc.) which have come in contact with an infected case. A more or less isolated group of individuals in fact offers an excellent opportunity for the intensive fighting of tuberculosis.

At the beginning of 1932 the medical and welfare services of N. V. Philips' Gloeilampenfabrieken commenced the systematic screening of all applicants for employment, and proposed the gradual extension during subsequent years of this examination to the whole staff of employees. The school children in the Philips schools had also to be included in this systematic investigation, followed by the families of patients.

The various groups submitted to periodical X-ray examination were:

- A) New employees.
- B) Existing staff.
- C) The schoolchildren.
- D) Employees' families.

A) *New Employees.* In addition to the ordinary medical examination, all new employees (above the age of 14 years) were submitted to screening. On the detection of any pathological abnormality this examination was supplemented by an examination of the blood, radiography, etc. Unsuitable and rejected applicants were reported to their own doctors or to the competent medical institution.

The results of this examination are given in Table I²⁾.

Table I. Incidence of Tuberculosis among New Employees.

	Active		Doubtful active
	Open	Latent	
Females	0.1 %	10 %	7 %
Males	3.8 %	4 %	12 %
Total	2.7 %	6 %	10 %

B) *Existing Staff.* In general all employees on engagement are submitted to a medical examination; subsequently to April, 1932, this examination was also supplemented by screening. It was, however, found that persons who originally exhibited

no foci on X-ray examination later developed a diseased condition of the lungs, thus indicating the extreme importance of periodical X-ray examination: It thus becomes necessary to examine all members of the existing staff by screening at regular intervals of, say, one to two years.

Persons showing pathological abnormalities in these routine examinations are submitted to closer examination; viz., general medical examination, blood tests and if necessary sputum tests, tuberculin reaction, and radiography. The examination shows whether the patient requires treatment (surgical, rest, hospital or sanatorium treatment) or merely observation (repeated blood tests and radiological examination) under favourable conditions of employment.

The family doctor is sent reports of these examination; a summary of the results achieved is given in Table II.

Table II. Incidence of Tuberculosis among Existing Staff

	Active		Doubtful active
	Open	Latent	
Females	0.9 %	4.2 %	9 %
Males	1.4 %	3 %	14 %
Total	1.27 %	3 %	13 %

Non-tubercular changes in the thoracic cavity, i.e. of the heart, vascular system, etc., were found to total 4 per cent in all cases examined in groups A) and B).

Table III shows the results obtained by systematic screening of all new applicants for employment; employees (approx. 10 000) engaged before April 1, 1932, were not screened during their initial examination, but all applicants subsequently engaged (approx. 5 000) were submitted to radiological examination.

Table III. Reduction in the number of tuberculosis cases among permanent staff since the introduction of radiological examination on April 1, 1932.

	Total	Examined	
		Before April 1, 1932	After April 1, 1932
Active	Open	14	13
	Latent	32	29
Doubtful Active		142	127
Total		188	169

C) *Schoolchildren.* Originally all children in Philips schools were screened once a year, but for practical

²⁾ Compiled by J. G. A. van Weel, Thesis, Utrecht, 1935.

reasons this periodical examination has now been limited to those children which give a positive reaction in the tuberculin test (Moro ointment). This reduces the number of children coming up for examination to about $\frac{1}{6}$ to $\frac{1}{7}$ of the total.

Results of these examinations were as follows: Of 1246 children of the Philips schools who were screened 1.2 per cent had active and 2.7 per cent doubtfully active symptoms. The former class thus required treatment and the latter careful observation.

D) Examination of Families. For the effective suppression of tuberculosis it is absolutely imperative to examine in addition to the patients all those persons coming in daily contact with them, either in their own homes or at works (apprentices, etc.), viz., the so-called "contacts".

For the periodical examination of these contacts the medical department of N.V. Philips has organised a consultative section for tuberculosis sufferers which works in collaboration with the local medical institution at Eindhoven.

The functions of the Philips consultative section include the examination of the following groups:

- 1.) Persons who report of their own accord complaining of symptoms, or who require examination as a precautionary measure (marriage) or those suspecting infection (open tuberculosis in the neighbourhood).
- 2.) Persons sent by their own physician owing to the detection of a lung disease.
- 3.) Persons sent by other employers to ensure that they are not suffering from an infectious lung disease (e.g. domestic employees).
- 4.) Contacts with all cases of active (open and latent tuberculosis) and with doubtfully active cases enumerated under A, B, C and D 1), 2) and 3).

The importance and necessity for treating or keeping under observation all contacts with tubercular patients is indicated by the fact that among contacts with patients suffering from active tuberculosis (open and latent) six times as many infections of all kinds were found than among the rest of the community, while among contacts with doubtfully active cases there were twice as many infected cases.

The ratio of the number of cases established by the active diagnosis of tuberculosis (systematic radiological examination of all members of the staff and their contacts) to the number of passive cases (sent by the patient's family physician or patient reporting of his own accord) is shown by

the proportion of cases passing through the consultative section which have been detected by each of the two methods. The relevant data are given in *Table IV*, which indicates that nearly three-quarters of all cases were detected as a result of direct examination.

Table IV. Distribution of cases according to method of detection

		Direct	Indirect
Active tuberculosis	Open	50 %	50 %
	Latent	70 %	30 %
Doubtfully active		77 %	23 %
Total		73 %	27 %

The great value of submitting large groups of persons to systematic radiological examination is shown by *Table V*, where the cases detected by radioscopy are compared with the number of cases diagnosed by family physicians and by the examination of contacts.

Table V. Value of Group Radioscopy for the detection of tuberculosis.

		Screening	Family physicians and examination contacts
Active tuberculosis	Open	36 %	64 %
	Latent	27 %	76 %
Doubtfully active tuberculosis		62 %	38 %

It may be concluded from this table that without routine screening of large groups of persons more than a third of the infections cases (open cases) would have remained undetected. Moreover, routine screening on these comprehensive lines reveals the greater part of the doubtfully active cases; this is particularly important since it is just these cases which provide the later active and open cases of

Table VI. Decrease in number of days of sick leave as a result of anti-tuberculosis measures.

Year	Average number of days of sick leave ³⁾
1932	1.38
1933	1.24
1934	1.21
1935	0.80

³⁾ Calculated per head and per annum with a maximum of 375 days of sick leave per head (including Sundays).

infection. By the periodical supervision of these cases the formation of unknown foci of infection can thus be, to a large extent, prevented.

It is interesting to note that during the periodical repetition of radiological examinations over a large mass of people the number of new cases detected gradually diminishes since all old

cases are already known and the families where the greatest danger of infection and spread of the disease obtains are kept under constant supervision by the consultative officials.

In conclusion *Table VI* gives data covering the period 1932 to 1935 which show the reduction in the average number of days of sick leave.

THE PHILIPS TWIN CURRENT WELDING UNIT

By H. A. W. KLINKHAMER.

Summary. A description of a unit for arc welding with direct current and alternating current is given. The transformer which feeds the rectifier during D.C. welding is used as a welding transformer during A.C. welding.

Introduction

Since some 5 years ago Philips first employed their hot-cathode valves in direct-current welding units the welding rectifier has continued to justify its place in welding practice. In these five years the wealth of practical experience gathered both in our own works and in other works has enhanced the reputation of this new unit, and a wide field of application has been developed in which the welding rectifier has shown itself as particularly apt and efficient.

These applications include:

- A) The welding of thin sheets from 0.02 to 0.1 inch thick, for which alternating current is not very suitable; thicker sheets also can be welded with direct current more quickly, easier and better than with alternating current especially if the direct current is furnished by a welding rectifier.
- B) Difficult welding work, such as vertical and overhead seams; direct current is the much more preferable for this purpose than alternating current.
- C) The welding of special metals, such as rustless steels, aluminium, and bronze. Aluminium cannot in fact be welded at all with alternating current.

For the welding jobs included under A) direct current of approx. 10 to 80 A is required; for B) and C) current intensities of up to 140 A are frequently needed and welding rods up to 0.15 inch in thickness used.

The applications of the welding rectifier are however not by any means limited to the above jobs for it can be used to advantage in all cases where a welding transformer is suitable. According to a large number of practical users work with the welding rectifier is more convenient and agreeable, and hence over long periods much more rapid. This is however to some extent purely a matter of individual taste, while the nature of the welding job also is a determining factor.

The welding rectifier competes with the welding transformer and the rotary converter. In the above enumeration under A), B) and C) of the specific fields of application of the welding rectifier, we had a comparison with the welding transformer particularly in mind. The jobs referred to can as a rule also be performed with direct current furnished by a rotary converter, but compared with the latter, the welding rectifier offers the important advantages of lower first cost and lower weight.

The speed with which a welding unit adapts its voltage to the rapidly fluctuating voltage of the arc is a point of paramount importance. Without entering into this question in great detail it may be recalled that during welding there is a continuous sequence of striking and re-striking of the arc. To strike the arc the point of the welding rod is brought into brief contact with the workpiece, which causes a powerful current to be built up, and is then removed from the surface again when the arc is struck. The length of the arc and hence also the minimum voltage for maintaining the arc

increase rapidly during this operation. There is now a race between the minimum arc voltage and the voltage output of the unit. If the voltage of the latter lags behind the arc breaks down and must be struck afresh. But with every collapse of the arc there is the danger of a weak spot being produced in the welded seam, so that it is absolutely essential to keep the voltage output of the supply unit continuously matched to the arc voltage.

It is just in this respect that the welding rectifier shows to better advantage than the welding converter. The unidirectional voltage furnished by the welding converter is in fact proportional to the field about the poles of the welding dynamo. This field cannot alter its magnitude abruptly, since any alteration in the field produces currents in the exciter winding and in certain circumstances also in the solid poles and yoke, which counteract a change in field. In the welding rectifier no similar lag is naturally found since no exciter winding is used.

There are various types of welding dynamo in which this lag is to a large extent eliminated by adopting a suitable circuit and appropriate lamination of the yoke and poles. But by these modifications in construction the cost of the converter is increased, although it can nevertheless never be made entirely comparable in efficiency with the welding rectifier.

The rapidity with which the voltage of the welding rectifier recovers after a short-circuit may be gathered from the oscillogram in *fig. 1*, which shows the variation in voltage when in a type 1306 Philips welding rectifier, the short-circuit current in the highest setting of the regulator is interrupted by a high-speed switch. It is seen that the time required for completely re-establishing the open-circuit voltage is less than 0.002 sec. An

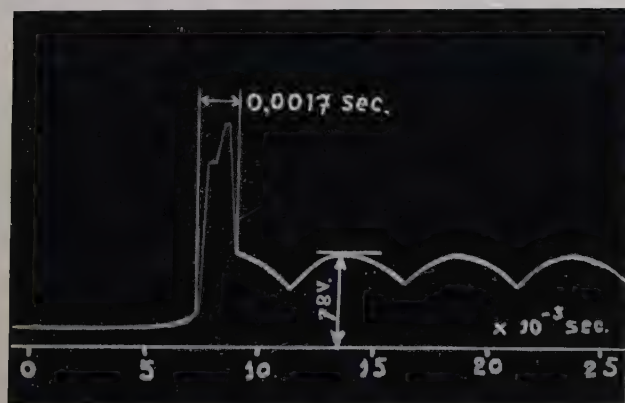


Fig. 1. Voltage oscillogram for Philips welding rectifier, type 1306, when suddenly interrupting the short-circuit current with a high-speed switch.

accurate time scale is here provided by the waves of the voltage oscillogram, and since four-phase rectification is employed each wave corresponds to 0.005 sec.

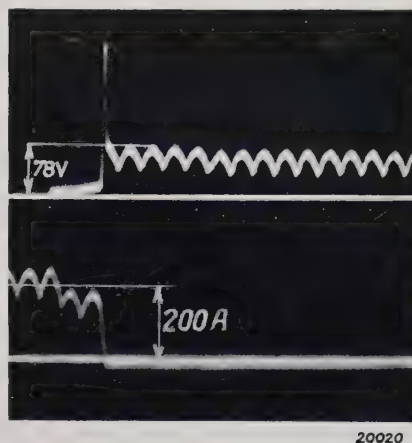


Fig. 2. Voltage and current oscillograms for the same operation as in *fig. 1* but registered at a slower film speed.

Fig. 2 reproduces a second oscillogram of the same operation, except that here the speed of the film, i.e. the time scale, is about five times smaller. The top curve represents the welding voltage, and the lower curve the welding current.

Philips Twin-Current Welding Unit

The special applications of the welding rectifier enumerated under A), B) and C) include only work which can be performed with comparatively low currents. At higher currents the welding rectifier frequently does not show to such good advantage as the welding transformer, and usually one of the latter type can be used quite satisfactorily.

Now a welding rectifier includes, in addition to the valves, also a transformer which is less efficiently loaded than as in normal circumstances. It thus seemed reasonable to adapt this transformer also for welding with high-intensity alternating current, especially as this would permit a considerable increase in the application of the equipment without entailing much extra cost.

These considerations led to the development of the twin-current welding unit, which can be used as a welding rectifier for lower currents and as a welding transformer for higher currents.

Circuit Layout of the Twin-Current Welding Unit

The unit is run off a three-phase mains supply. It is equipped with a switch, in one extreme position of which the unit operates as a welding rectifier and in the other extreme position as a welding transformer, while in the middle position

the output terminals are dead and all circuits are disconnected from the supply.

The unit contains two single-phase leakage transformers, whose leakage resistances can be simultaneously altered by adjusting a magnetic leakage regulator. This permits continuous variation of the welding current between wide limits.

If the switch is moved into the D.C. welding position, the primaries of the transformers are interconnected to a *T*-circuit, and they transform the three-phase mains current into low-voltage four-phase current which is then rectified by the thermionic valves.

In the A.C. position of the switch one pole of the three-phase mains supply is off circuit. The two single-phase transformers are then interconnected in parallel across the two other poles; the four secondary coils, which in the rectifier circuit constitute the arms of the four-phase star connection, are then interconnected in parallel and each carries one fourth of the welding current.

Fig. 3 shows a simplified circuit for the D.C. position of the switch. The points *U*, *V* and *W* are connected to the phases of the three-phase network and *H* is connected to *K*. The windings are dimensioned to give the vector diagram shown

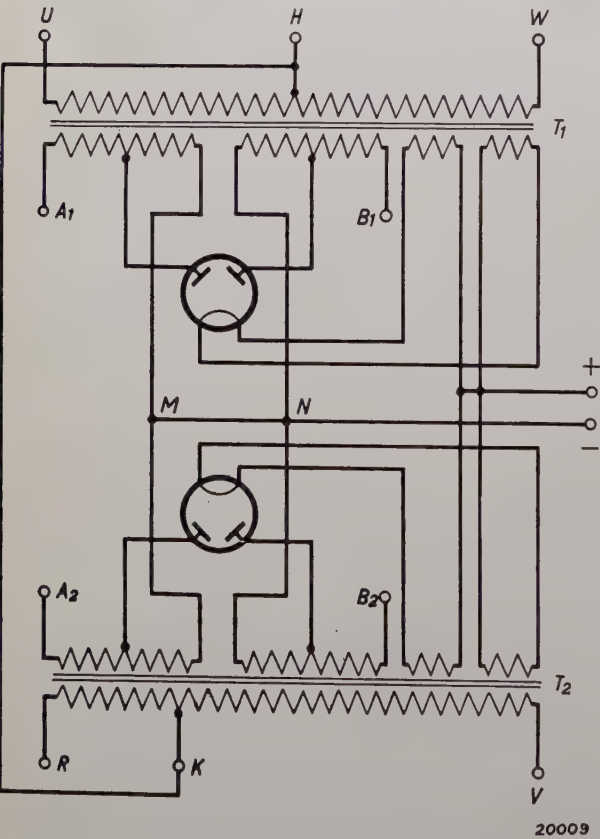


Fig. 3. General circuit layout for D.C. welding with the Philips twin-current welding unit.

in fig. 5a, and the *K*—*R* section of the winding remains dead. The secondary windings form a symmetrical four-phase star connection, whose neutral point is connected to the negative output terminal. The positive output terminal is connected to the centre of the heating windings, which surround the primary coils and whose voltage is therefore independent of the load.

On changing over to A.C. welding, the simplified circuit shown in fig. 4 is obtained. The points *H* and *K* of the primary winding are now no longer interconnected; but *U* and *R* are linked to each other, as well as *W* and *V*, and these terminals are connected to the delta voltage of the three-phase mains supply, so that the fields of the two transformers are in phase with each other and no longer have a displacement of 90 deg. as in the previous case (see fig. 5b). The left hand terminations of the four secondary windings are connected with one output terminal, and the right hand terminations with the other terminal. In this position of the change-over switch the D.C. windings are open-circuited, so that no D.C. power is unnecessarily wasted during welding with A.C. As indicated in the circuit diagram, the secondary windings

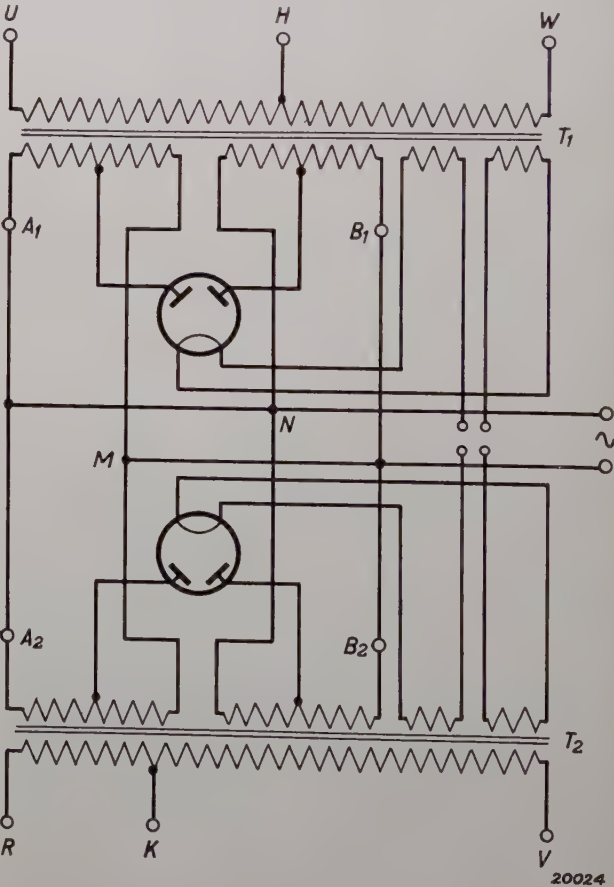


Fig. 4. General circuit layout for A.C. welding with the Philips twin-current welding unit.

in this circuit have been lengthened by several supplementary windings, such that the open-circuit voltage is raised to the value required for

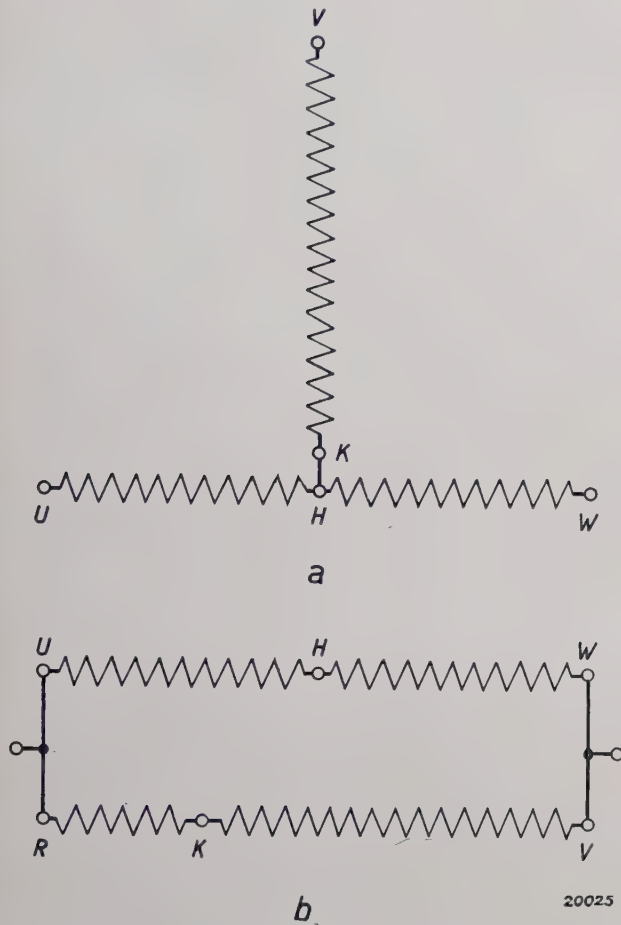


Fig. 5. a) Diagram of connections of primary windings when using the welding unit as a welding rectifier.
b) Diagram of circuits when using the welding unit as a single-phase transformer.

A.C. welding. These supplementary windings are wound above the primary coil, thus making the leakage resistance just equal to the value at which the unit furnishes alternating current at 300 A in the extreme outer position of the leakage regulator. This maximum value of 300 A was selected out of consideration of the practical need of obtaining efficient welding with sheathed welding rods 0.3 inch thick.

The primary winding is also provided with a number of taps not shown in the diagram, these permitting the unit to be connected to three-phases supplies of other voltages, e.g. 220 and 380 volts or 190 and 220 volts. Changing over from one voltage to the other is done by readjusting four small clips on a terminal board located under the cover.

Construction of the Transformers and the Regulator.

The use of leakage transformers in heavy-current technology introduces a number of difficulties which are the greater the larger the transformer used. If, for instance, an ordinary leakage transformer rated for several 10 kVA is enclosed in an iron housing, the powerful leakage field surrounding the transformer will induce eddy currents in the magnetic material of the housing, framework and constructional elements, these eddy currents being the direct cause of losses, overheating and humming of the iron structure. It therefore becomes necessary to make the framework and housing from expensive non-magnetic material, a method which has been adopted by various constructors of welding transformers using brass for the framework and wood for the housing.

A different method was adopted in the twin-current welding unit. Instead of making the transformers of the core-type as commonly adopted for units of this rating, the shell-type construction was favoured, although a little more material is perhaps entailed in this design of transformer. With this design the leakage field does not indeed constitute a source of disturbance, as may be seen from *figs. 6 and 7*.

Fig. 6 is a diagrammatic sketch of a leakage transformer of the core type, while *fig. 7* shows the same transformer of the shell type. Between the primary coil *I* and the secondary coil *II* is the magnetic shunt *C*, which in the core-type unit is of one piece and in the shell-type is in two pieces. To alter the leakage resistance it is sufficient to insert the shunt to a greater or less depth in the aperture, so that regulation is obtained by displacement perpendicular to the plane of the paper.

When the transformer is on load, then neglecting the magnetising current the ampere-turns on the primary coil are equal to those on the secondary. The two coils thus give the same magnetic field intensity; the direction of this intensity at a particular moment is shown by arrows in the figure. In *fig. 6* this produces a positive magnetic potential in the whole of the upper yoke *B* and a negative magnetic potential in the lower yoke *A*. The magnetic field strength at any surrounding point, e.g. at the point *P*, which is compounded of a component from each *A* and *B*, is readily seen to be of the same order of magnitude as the components themselves.

In *fig. 7*, however, the part *B* of the middle limb between the coils is separated from the surroundings by the shell *A* which may be regarded as a

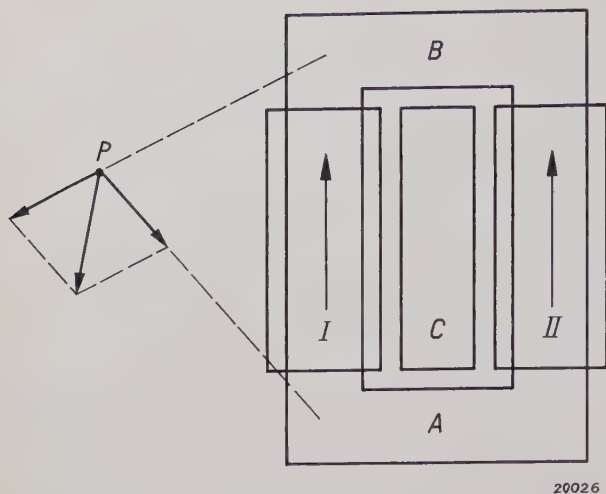


Fig. 6. Leakage transformer, core type.

magnetic short-circuiting ring. In this way the whole of the surroundings are completely screened from magnetic effects which may emanate from the transformer.

This does not, however, entirely apply to points outside the plane of the paper; nevertheless it is definite that the leakage field in the design shown in fig. 7 is concentrated to a greater extent towards the interior of the transformer than in the design shown in fig. 6. The difficulties with the core-type transformer mentioned above are not experienced with the shell-type, so that the frame and housing of the latter can without any apprehension be made of iron.

Nevertheless the core-type transformer with its powerful external leakage field could not be used here for an entirely different reason: In an experiment using two core transformers in the circuit shown in fig. 3 it was found that on load one rectifying valve carried almost double the current passing through the other valve, although the open-circuit voltages and the short-circuit currents were the same. The valves had exchanged their functions when the phase sequence of the mains supply was reversed. Although the currents could be balanced by increasing the distance between the transformers, this way out of the difficulty was naturally out of the question in a welding unit.

The cause of this behaviour is to be sought in the mutual influence of the transformers produced by their leakage fields, as a result of which transformer T_1 generates a supplementary voltage $-jkI_1$ in the secondary winding of T_2 and T_2 a supplementary voltage $-jkI_2$ in the secondary winding of T_1 . Here k is a coefficient of mutual induction. If each transformer has a leakage resistance jx and carries a load of resistance R ,

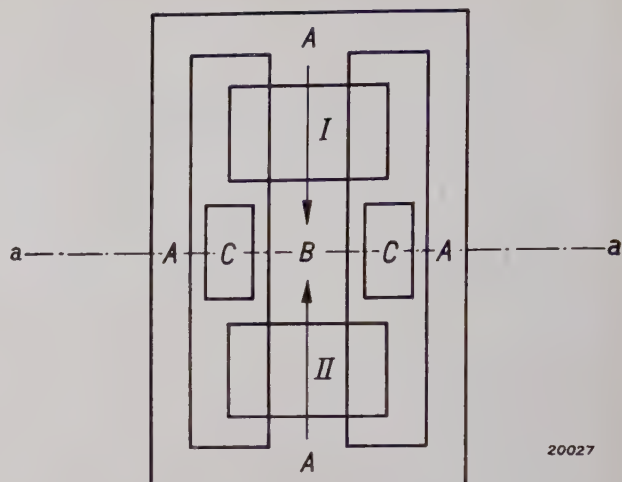


Fig. 7. Leakage transformer, shell type.

and V_1 and V_2 are the open-circuit voltages, then the equations for the two circuits are found to be:

$$\begin{aligned} V_1 &= jxI_1 + RI_1 + jkI_2 \\ V_2 &= jxI_2 + RI_2 + jkI_1 \end{aligned}$$

If the first equation is multiplied by j and is then subtracted from the second equation, then since $V_2 = jV_1$ we get:

$$\frac{I_2}{I_1} = j \frac{R + jx - k}{R + jx + k}$$

i.e. $I_2 \neq jI_1$ for $k \neq 0$, in other words we get an asymmetrical three-phase load when the transformers influence each other through their leakage fields. On short circuit ($R = 0$), although the currents are equal, the phase difference is yet not equal to 90 deg. With the shell-type transformer k was found to be so small that the valve currents were practically equal, also when the unit was on load.

If the secondary circuits are not kept separate as in the above example, but are coupled together on the D.C. side of the valves, this factor can be taken into consideration by assuming that one transformer carries a load R_1 and the other a load R_2 , where $R_1I_1 = R_2I_2$. Calculation is then not so simple but gives the same qualitative result.

The shell type of transformer also offers advantages as regards the construction of the regulating device. To make a movable magnetic shunt is never a simple matter, since powerful magnetic forces have to be taken into consideration. Thus with an air gap with an induction B , the force acting on the contiguous iron surfaces is $B^2/25000$ gr per sq. cm, i.e. approx. 600 kg per sq. dm with an induction of 12000 gauss. With a mains frequency of 50 cycles this force fluctuates 100 times per second between zero and its maximum value.

Owing to the elastic response of the structure a loud hum is then very quickly produced, particularly where the whole structure does not constitute a rigid unit, and the magnetic shunt has to be made to slide along the guide bars.

Although in the design shown in figs. 6 and 7 the magnetic forces which act on the shunt regulator have indeed been compensated theoretically, yet high unbalanced magnetic forces immediately make their appearance in service owing to small discrepancies in erection, such as a slight twist of the regulator about its axis perpendicular to the plane of the paper.

The whole construction has therefore to be made extremely rigid. Heavy guide bars must be used whose supports in their turn must be very rigidly connected to the transformer.

In order not to make the unit excessively costly, another method was adopted which although suitable for the shell type was not applicable to the core type of transformer: it consisted of clamping the shunt cores after adjustment firmly against the middle core. During service they then form a rigid aggregate with the middle core, so that the magnetic forces acting between the shunt cores and the middle core produce no displacement and hence also no hum is heard.

To illustrate this the section *a—*a** in fig. 7 is

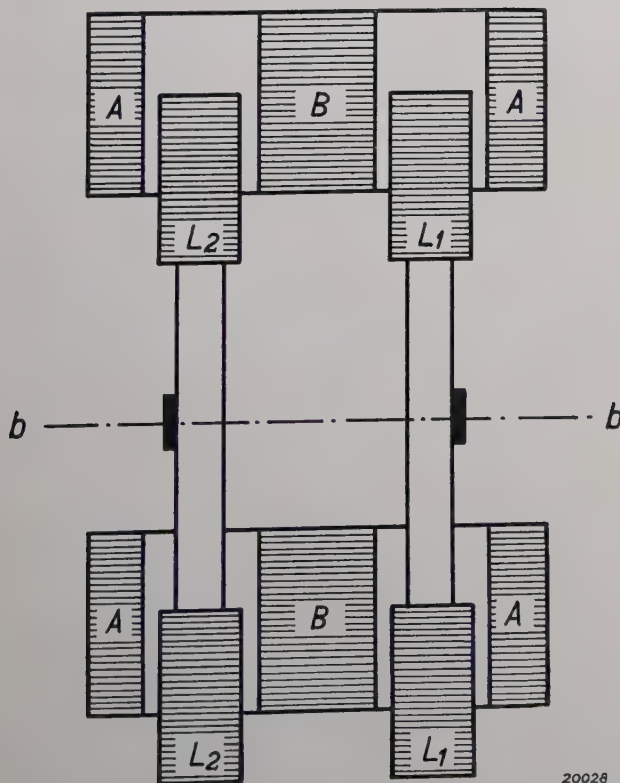


Fig. 8. Leakage transformer with locking-type regulator (section through *a—*a** in fig. 7).

shown in fig. 8. The middle cores are denoted by *B*, the outer cores by *A*, and the hatching indicates the direction of the laminations. The two shunt cores *L1* are made up of sheets packed on a brass rod with the same thickness, and so combined to form a rigid bar. The two shunts *L2* are constructed on similar lines. To adjust the welding current these bars are displaced longitudinally and then clamped against the middle core by a bolt whose axis is indicated by *bb* in the figure.

The Twin-Current Welding Units, Types 1306 and 1307

Two types of welding units have been built to date on the principles outlined above, viz., 1306 (fig. 9) for high outputs and 1307 (fig. 10) for low



Fig. 9. Twin-current welding unit, type 1306. The lever change-over switch serves for changing over from alternating to direct current. The current intensity is regulated by means of the upper handwheel; the magnetic shunt cores are clamped against the middle core by means of the side handwheel.

outputs. The welding current can be regulated between the following limits:

Type 1306: Direct current 25—140 A.
Alternating current 60—300 A.

Type 1307: Direct current 10—80 A.
Alternating current 30—175 A.

The D.C. range of type 1306 is suitable for the duties enumerated under A) above, viz., on sheets of 0.04 inch thick upwards, also for the work given under B and C using welding rods up to 0.15 inch thick. With alternating current welding rods up to 0.25 inch thick can be employed with this unit.

In type 1307 the D.C. range will permit welding on sheets from 0.02 inch thick upwards, as well as the use of welding rods up to 0.1 inch thick. With alternating current welding rods up to 0.15 to 0.2 inch thick can be used with this unit.

Type 1306

The type 1306 welding unit is shown in fig. 9. It is of rainproof design and mounted on two wheels with solid rubber tyres; fan cooling is provided. The housing is in the form of a cylindrical wind tunnel in which the two transformers are mounted one behind the other and behind the two type



Fig. 10. Twin-current unit, Type 1307. The side lever serves for adjusting the current, while changing over from alternating to direct current is performed by means of the switch B on the cover. The clamping arrangement is operated by means of the crank A.

1069 valves; the latter are fixed side by side in a light frame held in a spring suspension. Then follows the fan which forces out the hot air through louvres on the pusher bar side. On the side of the housing is a semi-cylindrical cover under which the change-over switch is situated, whose top, middle and bottom positions correspond to alternating current, “off”, and direct current.

The handwheel on the top side serves for adjusting the welding current; through a vertical shaft and gearwheel and rod it controls the magnetic shunts which can be displaced in the axial direction of the cylindrical housing. A pointer is attached to the handwheel to indicate the welding current on a scale.

The handwheel at the side of the housing operates

the clamping arrangement; on a complete revolution the shunt cores are clamped tight against the middle core.

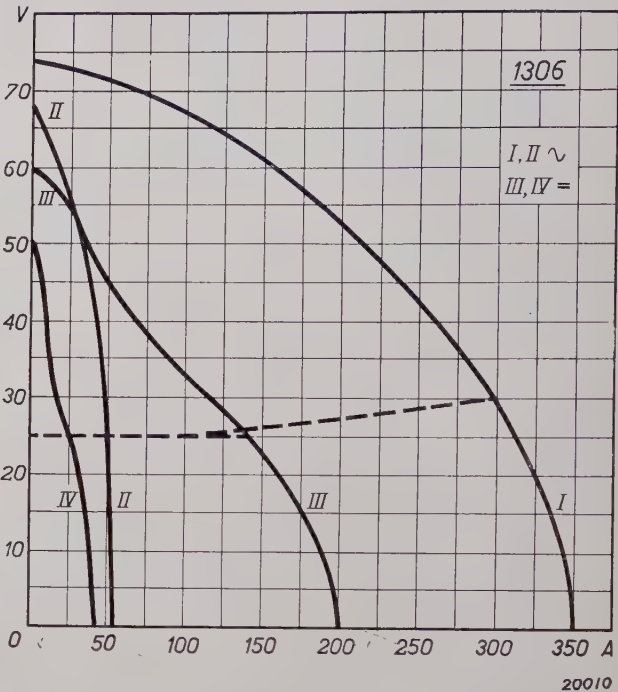


Fig. 11. Current-voltage characteristics of the twin-current welding unit, Type 1306.

- I . on adjustment to highest alternating current,
- II " " " lowest " "
- III " " " highest direct "
- IV " " " lowest " "

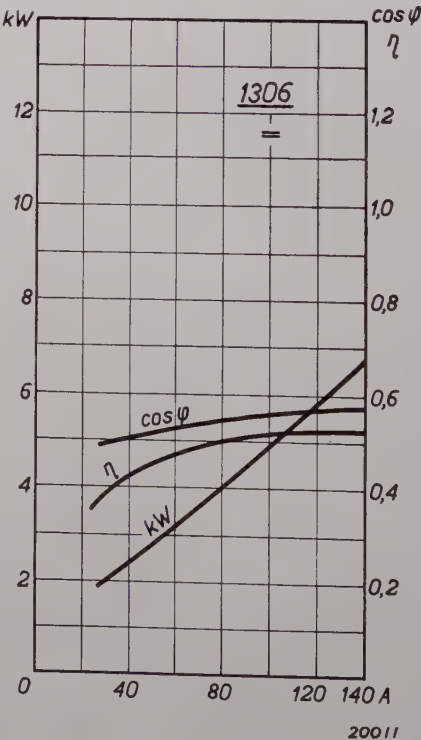


Fig. 12. Curves for the efficiency, power factor and power consumption of the twin-current welding unit, type 1306, used as welding rectifier for an arc voltage of 25 volts.

To inspect the interior the carrying ring is screwed off, the handwheel detached, the clips at the side opened and the upper part of the housing which is hinged to the lower half is tilted upwards.

Fig. 11 shows the static volt-ampere characteristics of the unit in the two extreme positions

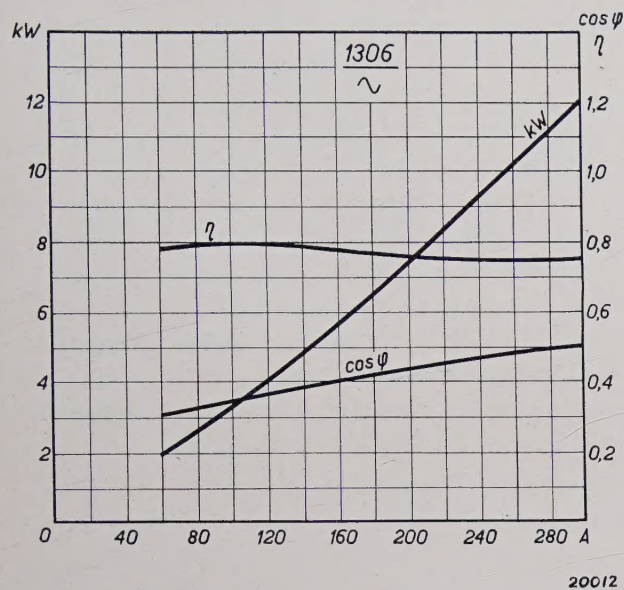


Fig. 13. Curves for the efficiency, power factor and power consumption of the twin-current welding unit, type 1306, used as welding transformer with an arc voltage varying from 25 to 30 volts along the broken line in fig. 11. Where a reduction in mains current consumption is desired, the power factor can be improved with the aid of a condenser.

of the regulator; curves *I* and *II* are those for the A.C. circuit and curves *III* and *IV* those for the D.C. circuit. Fig. 12 gives a few D.C. curves and fig. 13 the corresponding curves for A.C.

Where it is desirable to reduce the power consumption from the mains, the power factor can be improved by means of a condenser.

Type 1307

A view of the type 1307 welding unit is shown in fig. 10. This type is splashproof and can be carried short distances by means of the handles. It is not provided with a fan but is designed for natural air cooling. The construction of the transformers and the regulator is exactly the same as in the 1306 type, except that the shunt regulator is not controlled by means of a gearwheel but by two forked levers. These levers are pivoted on the level of the base where they are attached to a horizontal shaft. The shaft can be turned from the outside through about 50 deg by means of a lever, which is shown in the figure at the front of the unit. The crank *A* on the cover of the unit actuates the clamping arrangement, and the crank *B* operates the changeover switch. The two valves of type 1054 are mounted above the transformers.

The characteristics and the curves for efficiency and power factor are very similar to those for type 1306.

ABSTRACTS OF RECENT SCIENTIFIC PUBLICATIONS OF THE N.V. PHILIPS GLOEILAMPENFABRIEKEN

- No. 1098:** H. van der Tuuk: Moderne Röntgentechniek (Ned. T. Natuurk. 3, 129 to 140, May, 1936).

This paper surveys the principal stages in the development of X-ray technology during recent decades. The requirements are set out which X-ray tubes for diagnosis and therapy have to fulfil.

- No. 1099:** F. M. Penning De beweging van electronen in een homogeen electrisch en homogeen magnetisch veld (Ned. T. Natuurk. 3, 141 to 154, May, 1936).

The author discusses the equations of motion of an electron under the action of a homogeneous electrical and a homogeneous magnetic field. If two long plates parallel to each other are employed as cathode and anode, then at a minimum angle φ between the magnetic field and these plates part of the electrons deflected by the magnetic field will not return to the cathode. For a number of special cases this angle φ is calculated from the magnetic field strength, the electrical field strength and the components of the velocity of emergence. The results are applied to gas discharges at a very low pressure in a magnetic field.

- No. 1100:** J. L. Snoek: Action of an alternating magnetic field on disks made of magnetic steel (Physica, 3, 361 to 370, June, 1936).

The author has observed that small disks of magnetic steel rotated in an alternating magnetic field situated parallel to the plane of the plates are subject to an accelerating moment even if the initial velocities are extremely small, until finally their revolution synchronises with the 50-cycle alternating field. This lability phenomenon is due to ferro-magnetic hysteresis and only occurs when amplitude of the magnetic field strength is of the same order of magnitude as the coercivity. The equations deduced are confirmed quantitatively. The lability also continues to occur at 500 cycles.

- No. 1101:** Balth. van der Pol: On potential and wave functions in n dimensions (Physica 3, 385 to 392, June, 1936).

Analogous to the derivation of the wave equation in n dimensions from one in $n + 1$ dimensions, by making the latter independent of one of the

dimensions concerned ("méthode de descente" of Hadamard), the same solutions can also be arrived at by means of problems in $n - 1$ dimensions ("méthode de montée"). This gives a simple method for deriving the classical Whittaker potential and wave functions in three dimensions in a generalised form and at the same time constitutes an extension of these functions to n dimensions. The integral expressions so derived also cover the Hankel functions and spherical functions of the second degree.

- No. 1102:** Balth. van der Pol: A generalization of Maxwell's definition of solid harmonics to waves in n dimensions (Physica 3, 393-397, June, 1936).

A solution of the potential equation in three dimensions derived by Maxwell with the aid of spherical functions is generalised for n dimensions and also for the wave equation, by the derivation of analogous solutions containing Bessel and Gegenbauer functions.

- No. 1103:** J. F. H. Custers and J. H. de Boer: Die Lichtabsorption des absorbierten Paranitrophenols (Physica 3, 407 to 417, June, 1936).

As already demonstrated for the adsorption of paranitrophenol by CaF_2 , adsorption at a BaF_2 surface also takes place in two different layers. The molecules of the lower layer are linked electrostatically with their OH dipoles to the fluorine ions of the surface. They have an absorption spectrum which compared to that of pure paranitrophenol is displaced considerably towards the red, the displacement being greater with BaF_2 than with CaF_2 . The molecules of the upper layer are linked to the molecules of the lower layer by Van der Waals's adsorption forces. The absorption spectrum has also undergone slight modification and shows a displacement towards the red, which diminishes as the concentration at the surface rises.

- No. 1104:** J. L. Snoek: Magnetic and electrical properties of the binary systems $\text{MO.Fe}_2\text{O}_3$ (Physica 3, 463 to 483, June, 1936).

The magnetic and electrical properties of the binary systems $\text{MO.Fe}_2\text{O}_3$ composed of ferric

oxide with ferrous, manganese, cupric, nickel or magnesium oxide are investigated. In addition to the two existant methods for distinguishing a homogeneous phase from a two-phase system a third method is also employed in which the demagnetising factor is derived from the so-called ideal curve. In this way it is possible to detect quite easily the presence of extremely small admixtures of a second nonmagnetic component. If as a result of the energy differences being too small segregation takes place very slowly, this method is of marked value (nickel and magnesium ferrite). Close to the Curiepoint (manganese ferrite) the deductions to be drawn from the measurements made are not conclusive, so that the method cannot be used in these cases. The results obtained coincide with those deduced from radiographs.

No. 1105: W. Elenbaas: Übergang der laminaren in turbulente Konvektions-Strömung im Hochdruckentladungsrohr (Physica 3, 484 to 490, June, 1936).

If the pressure of the diameter of a high-pressure mercury discharge exceeds a certain value, the discharge becomes unstable. It is observed that convection flow which is initially streamline then becomes turbulent. With diameters exceeding 10 mm, the amount of mercury per cm of tube length at which instability occurs, expressed as a function of the cross-section, conforms with the laws of similitude for turbulence. The Reynolds's number calculated herefrom is of the order of 1000, which indicates that the phenomenon is in fact caused by turbulent convection flow.

No. 1106: A. A. Kruithof and F. M. Penning: Determination of the Townsend ionisation coefficient α for pure Argon (Physica 3, 515 to 533, June, 1936).

For determining the Townsend ionisation coefficient a new apparatus has been evolved which can be evacuated at a high temperature and on which exterior to the tube an arrangement has been fitted for displacing the cathode. The ionisation coefficient α of pure argon was determined for values of the quotient of the electrical field strength in volts per cm and the gas pressure in mm of mercury (reduced to 0 C°) between 5 and 400 volts per cm per mm. For small values of this quotient the values obtained were about 500 times smaller than stated by Ayres.

No. 1107: F. M. Penning: Verzögerungen bei der Zündung von gasgefüllten Photo-

zellen im Dunkeln (Physica 3, 563 to 568, June, 1936).

In certain gasfilled photo-electric cells, spontaneous discharge in the dark only takes place with a specific lag depending on the voltage employed. Very weak illumination reduces this delay considerably. Owing to the thermal emission of the cathode a current flows through the cell already at voltages which are under the starting voltage. This current has a specific discontinuous characteristic which may be ascribed to the window of the cell acting as a third electrode with a powerful secondary emission. If the previous discharge is given due consideration, it is found that the duration of the lag diminishes with increasing temperature of the photo-electric cell.

No. 1108: E. J. W. Verwey and J. H. de Boer: Molecular energy of alkali halides. (Rec. Trav. chim. Pays-Bas 55, 431 to 442, June, 1936).

The lattice energies of the alkali halides and the dissociation energies of the halide molecules into ions are recalculated, the values of Mayer and Helmholtz being corrected by the subsequent more accurate estimation of the Van der Waals and London forces given by Mayer. The electron affinities are then found to be: F⁻ 92.2; Cl⁻ 83.0; Br⁻ 77.2, and I⁻ 69.9 kg. cal. The dissociation energies of the molecules which are deduced from lattice and sublimation energies are compared with various values deduced from molecular models (Preis, Born and Heisenberg). In place of the law of powers the exponential law is employed for the repulsion in calculating the dissociation energy, consideration also being given to the polarisation energy. If the six immediately surrounding ions are alone taken into consideration calculation is much simplified and very little difference is found in the results. In the case of molecules with nuclear distances smaller than 2 Å considerable deviations are found from the exponential law of repulsion. The calculated proportions of the polarisation energy in the linkage are as expected several kgcal too high, assuming homogeneous fields and constant polarisability.

No. 1109: J. H. de Boer and E. J. W. Verwey: Energy and structure of the molecules of the alkaline earth oxides. (Rec. Trav. chim. Pays-Bas 55, 443 to 450, June, 1936).

With the aid of Born and Mayer's exponential law of repulsion, the lattice energies of the

oxides BeO, MgO, CaO and BaO have been recalculated. The electron affinity of oxygen ($O-O^{--}$) was thus found to be -173 kcal per gramatom. As for the alkali halides the molecular energies were also calculated for these oxides. The values obtained for ionic molecules are considerably less than those calculated from the lattice and sublimation energies, which indicates that the homopolar linkage has a marked effect on the combination energy. It follows from other considerations that the oxides of the alkaline earths although they undoubtedly form ionic lattices have a predominating homopolar valency in the vapour state and then form atomic molecules.

No. 1110: J. H. de Boer, P. Clausen and J. D. Fast: The α - β transition with mechanically-treated and with untreated zirconium (Rec. Trav. chim. Pays-Bas, **55**, 450 to 458, June, 1936).

In 1926 Zwicker observed a transition stage with zirconium wires between temperatures of 1100 and $1400^\circ C$; later investigations showed that there was a sharp transition temperature. In the present paper it is shown that the ill-defined character of the α - β transition in the earlier investigations was due to the heating of the material in different stages of working. The transition temperature was $865 \pm 10^\circ C$. The total radiation of β zirconium is proportional to $T^{4.7}$.

No. 1111: J. H. de Boer and J. D. Fast: The influence of oxygen and nitrogen on the α - β transition of zirconium (Rec. Trav. chim. Pays-Bas, **55**, 459 to 467, 1936).

In zirconium two or more atoms per cent of oxygen and nitrogen can be homogeneously absorbed. The transition from hexagonal α zirconium to the regular β modification does not then, however, take place at a well-defined transition temperature of $865 \pm 10^\circ C$., but throughout a wide transition range. The transition commences at 10 atoms per cent of oxygen at a temperature of $910^\circ C$. and is not yet completed at $1550^\circ C$. A low-oxygen β -phase is in this range always in equilibrium with a high-oxygen α -phase. The resistance of a specific test-bar was found to be free from hysteresis phenomena and to depend only on the temperature. If the zirconium absorbs oxygen and nitrogen at the same time, the resistance as a function of the temperature exhibits definite hysteresis phenomena. The resistance curves are practically unaffected by the addition of aluminium.

No. 1112: J. A. M. van Liempt: Die Dampfdrücke des Bariums (Rec. Trav. chim. Pays-Bas, **55**, 468 to 470, June 1936).

From the careful vapour-pressure measurements carried out by Rudberg and Lampert on barium between 500 and $750^\circ C$., the author has calculated the sublimation pressure and the sublimation velocity as a function of the temperature, using the formulae previously derived by him in another paper (No. 1051). Employing a formula also from a previous paper (No. 1068), the velocity of vaporisation in an inactive gas can now also be calculated.

No. 1113: E. J. W. Verwey and J. H. de Boer: Cation arrangement in a few oxides with crystal structures of the spinel type (Rec. Trav. chim. Pays-Bas, **55**, 531 to 540, June, 1936).

On the basis of the differences in character of the cations and in their arrangement over the crystal lattice, it is possible to account for the good conductivity for electrons possessed by Fe_3O_4 and the absence of such conductivity in Co_3O_4 and Mn_3O_4 . From radiographic measurements it is concluded that Fe_3O_4 consists of divalent and trivalent ions and Co_3O_4 and Mn_3O_4 of divalent and tetravalent ions. The lattice of Fe_3O_4 is an abnormal spinel type in which probably all Fe^{++} together with half the Fe^{+++} are distributed statistically over mutually-equivalent crystallographic lattice points. Co_3O_4 and Mn_3O_4 have a normal spinel lattice: $Co^{IV}Co^{II}_2O_4$ and $Mn^{IV}Mn^{II}_2O_4$. The Mn_2O_3 prepared as described by Dubois is γ - Mn_2O_3 . Its face-centred tetragonal cell may be regarded as a deformed elementary cell of γ - Fe_2O_3 type. Contrary to Mn_3O_4 it contains only trivalent cations, similar to γ - Fe_2O_3 .

No. 1114: E. J. W. Verwey: De electrolytische dubbellaag van kolloiden, in het bijzonder van AgI, metalen en kool γ (Chem. Wbl., **33**, 414 to 420, June, 1936).

In this report of a paper read, several fundamental problems in the theory of the electrical double layer are discussed, viz., those relating to the structure of the inner and outer surfaces of the double layer, their production, and the part played therein by differences in the contact potentials in the boundary layer. The examples discussed include the negatively charged dialysed AgI sol, the electro-kinetic behaviour of rare metals in water, and the behaviour of positive and negative carbon suspensions.